The LTP interferometer and Phasemeter

Gerhard Heinzel

on behalf of the Optical Bench team:
Albert-Einstein-Institut Hannover,
University of Glasgow,
EADS Astrium Immenstaadt,
Rutherford Appleton Laboratories Chilton,
TNO TPD Delft,
ESTEC Noordwijk

5$^{\text{th}}$ International LISA Symposium,
ESTEC, July 12, 2004.


EADS
ASTRIUM
Albert-Einstein-Institut Hannover

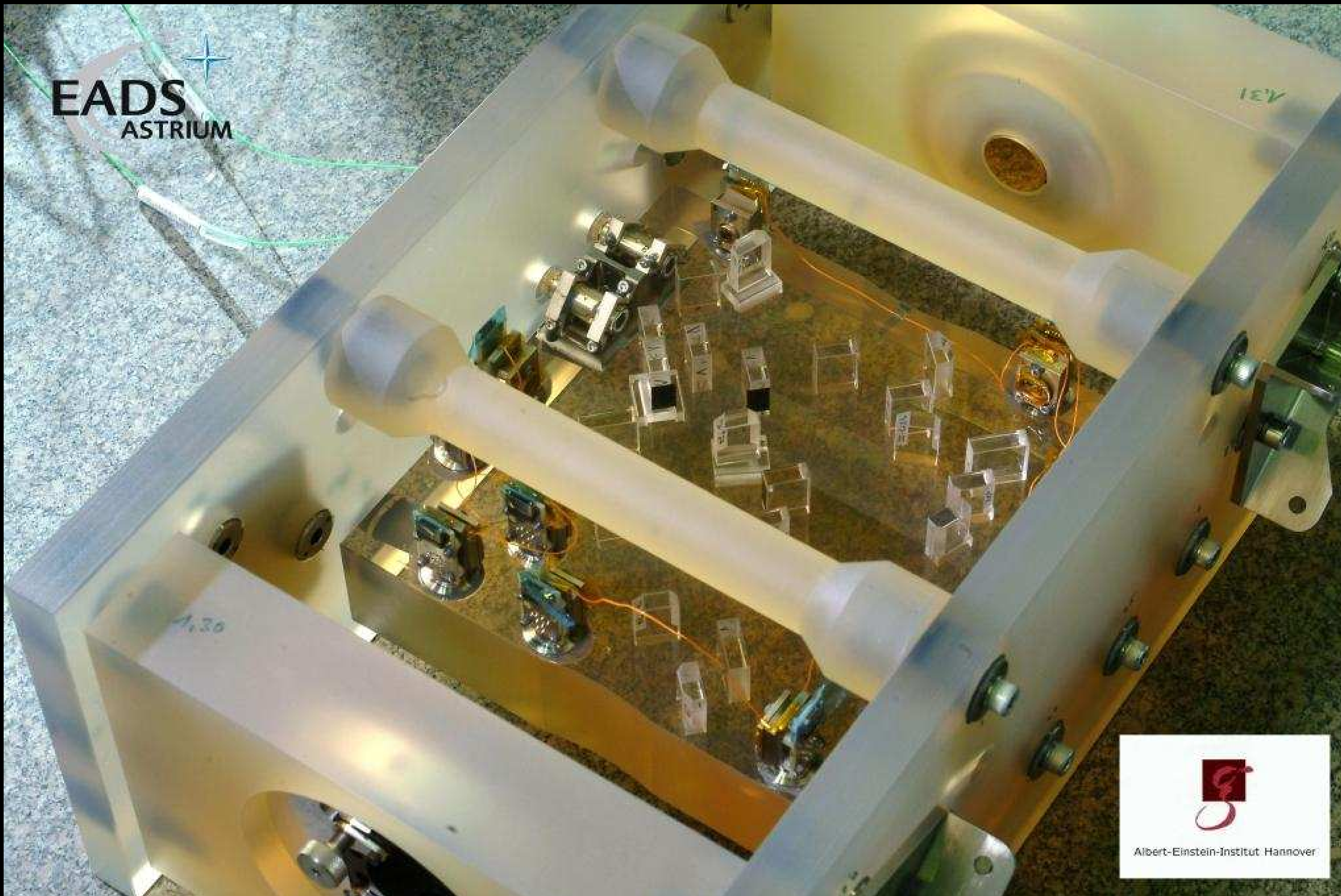
EADS
ASTRIUM
Albert-Einstein-Institut Hannover

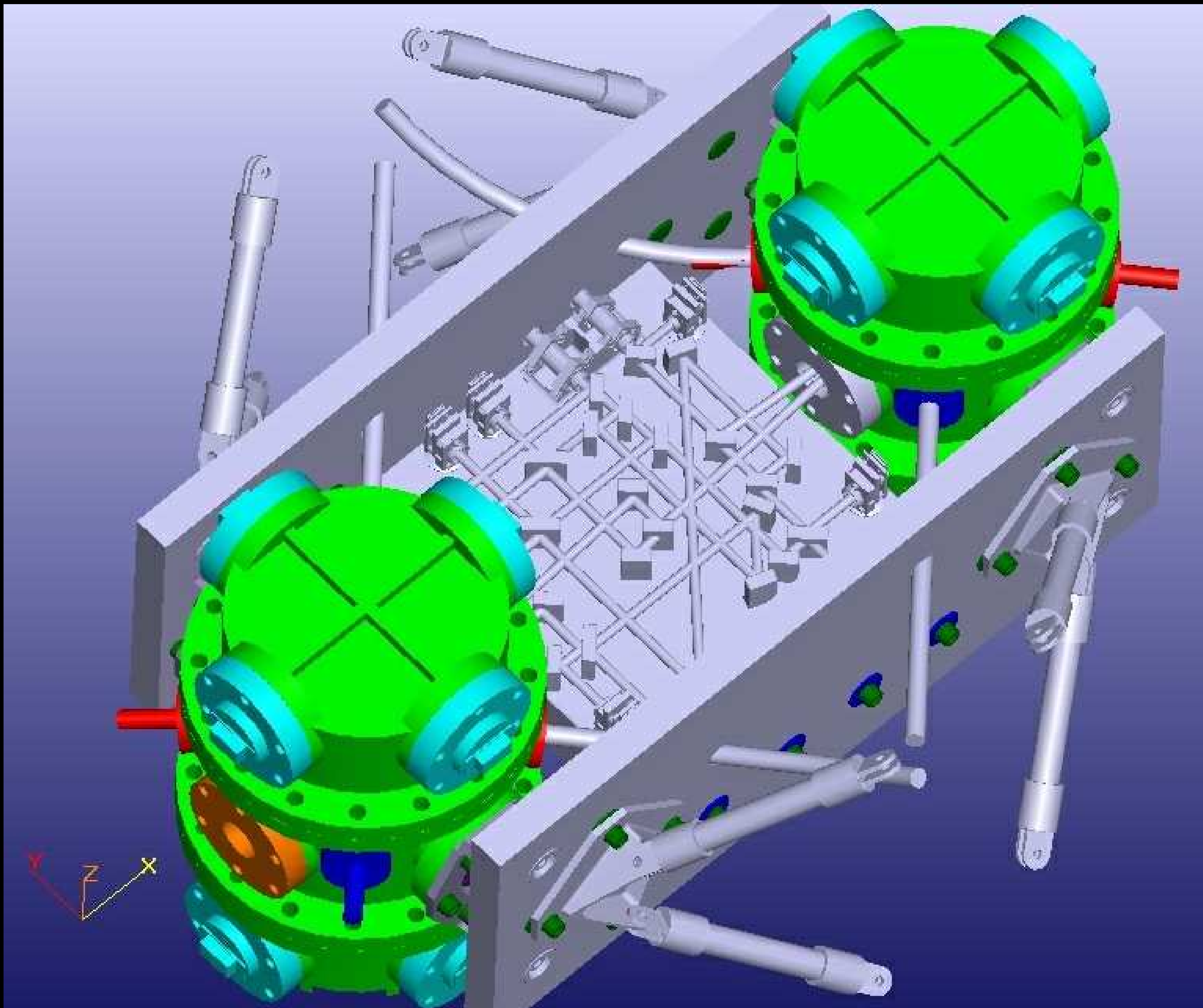

Y
Z
X

Heterodyne Mach-Zehnder interferometer

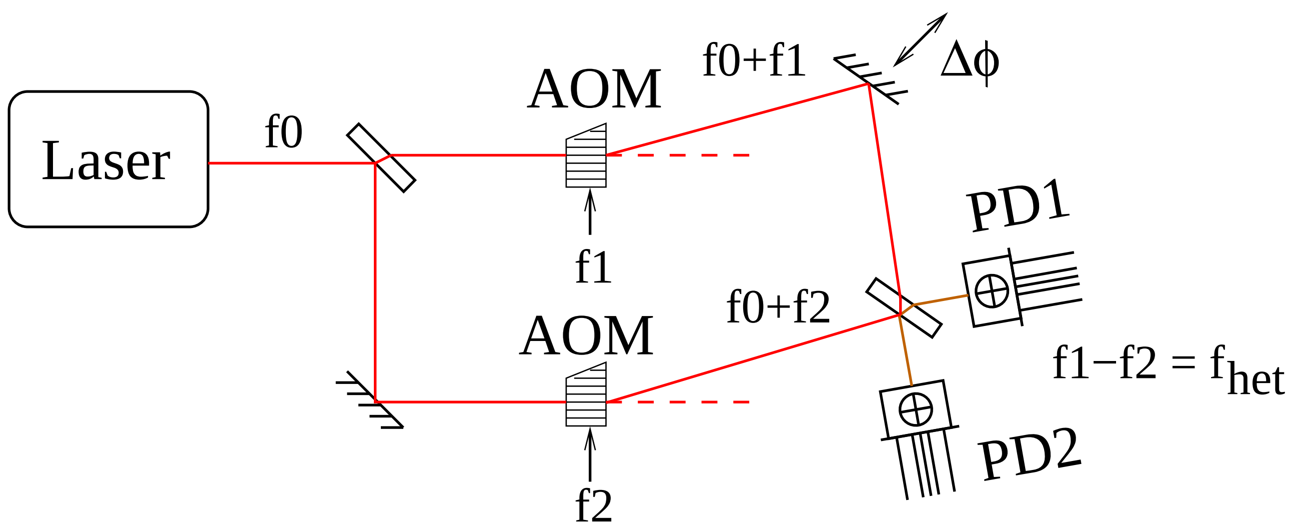

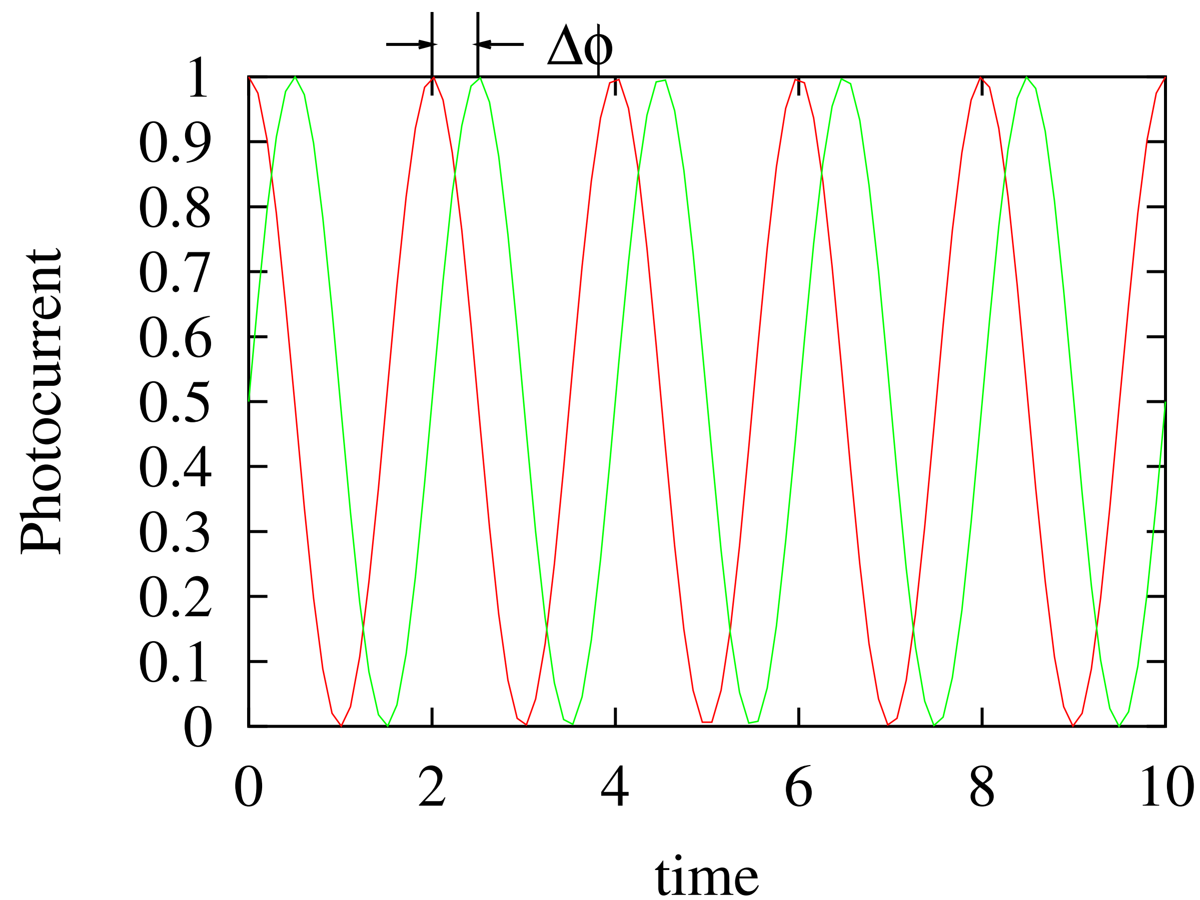

It has constant sensitivity over a range of $> \pm 100\,\mu$m. The heterodyne frequency f_{het} is a few kHz (1.6 kHz in the EM).

Interferometer budget

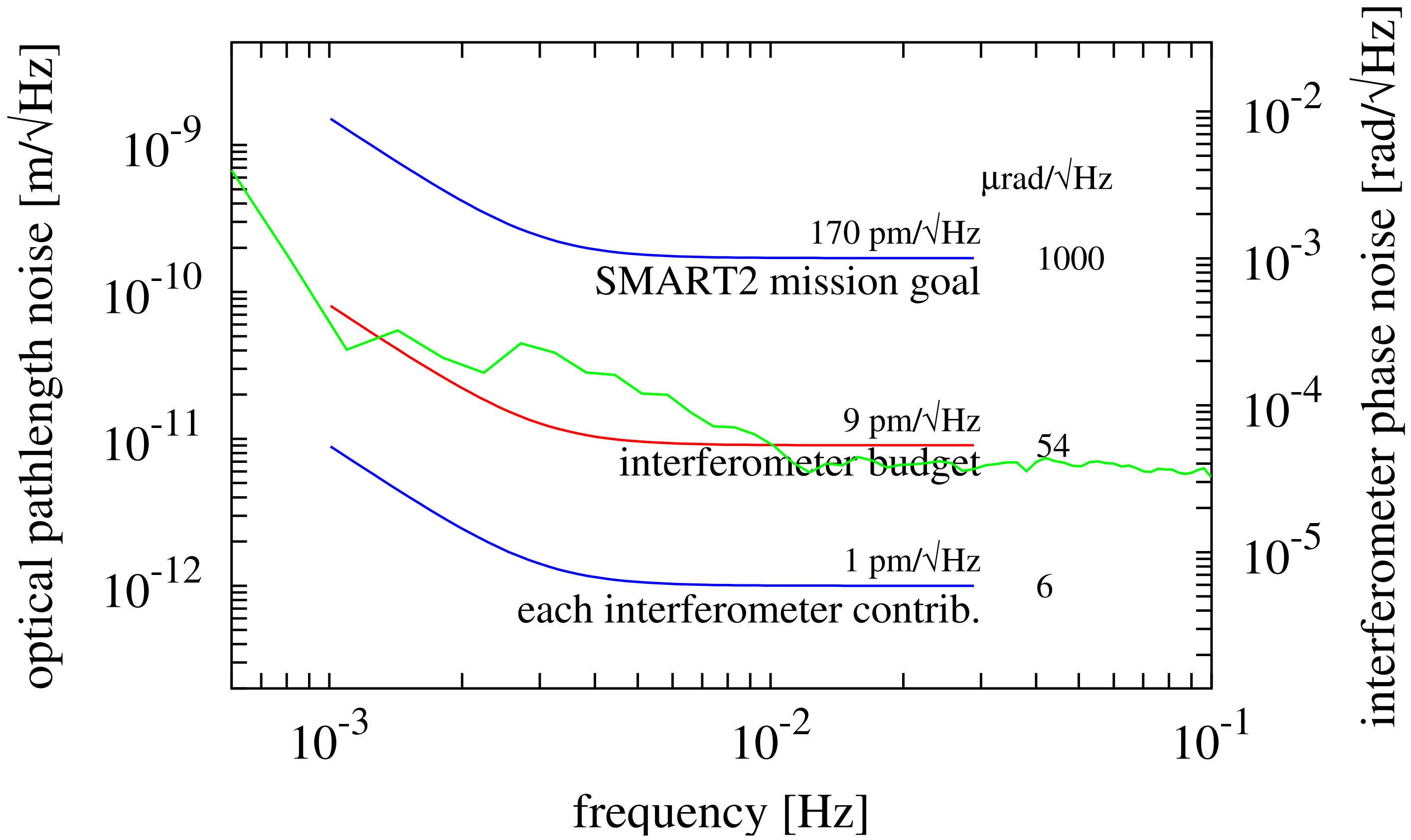

Note the new interpretation. As compared to some earlier versions, nothing has changed for the interferometer budget, which is, however, now a factor of nearly 20 below the mission goal.

The frequency dependence of all interferometer-related budgets is

$$y(f) = y(30\,\text{mHz}) \cdot \sqrt{1 + \left(\frac{3\,\text{mHz}}{f}\right)^4},$$

and all budgets in the following are given at 30 mHz (such as $9\,\text{pm}/\sqrt{\text{Hz}}$ for the interferometer).

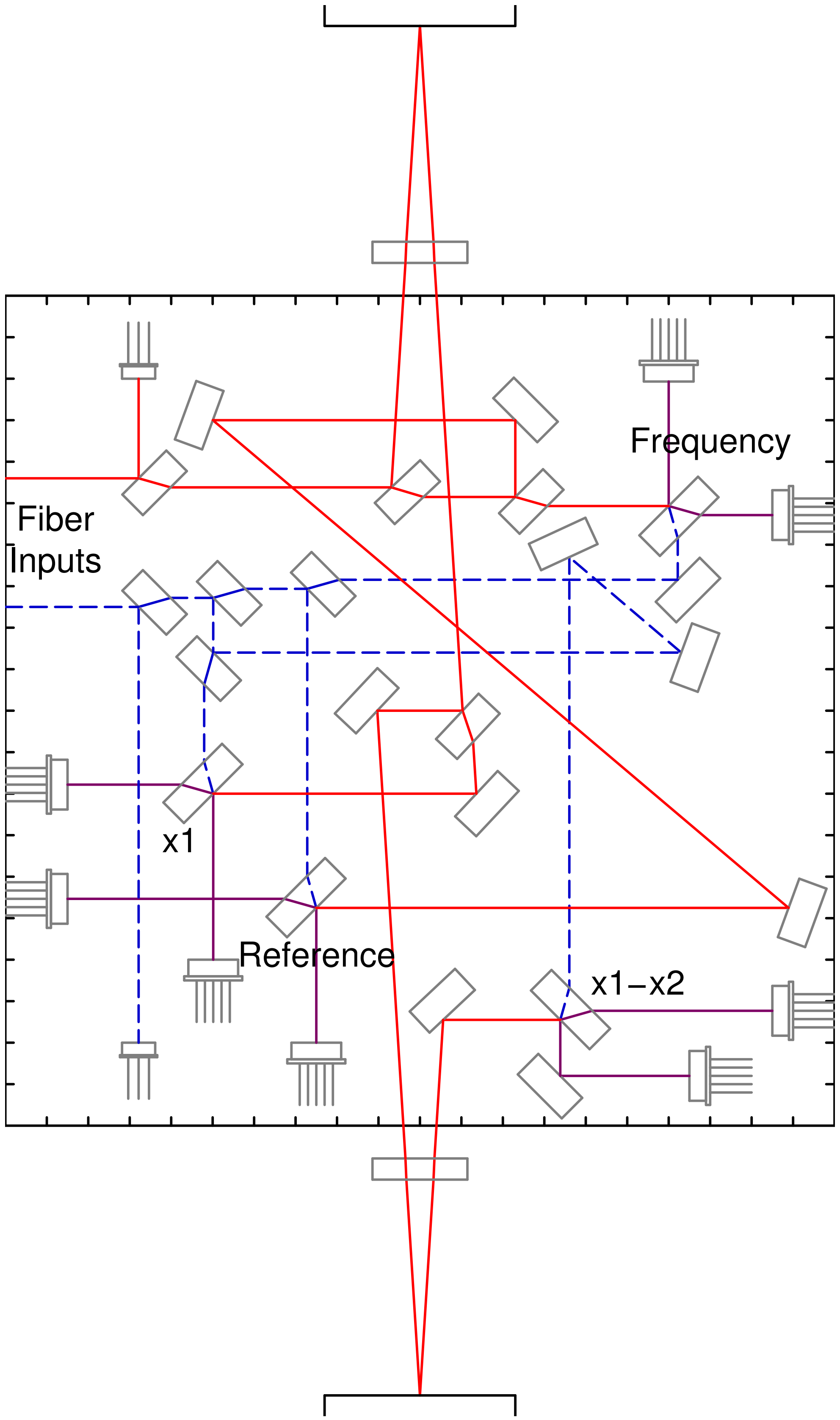

4 interferometers:

$x_1 - x_2$ provides the main measurement: the distance between the two test masses and their differential alignment.

x_1 provides as auxiliary measurement the distance between one test mass and the optical bench and the alignment of that test mass.

Reference provides the reference phase for $x_1 - x_2$ and x_1.

Frequency measures laser frequency fluctuations with intentionally unequal pathlengths.

$x_1 - x_2$

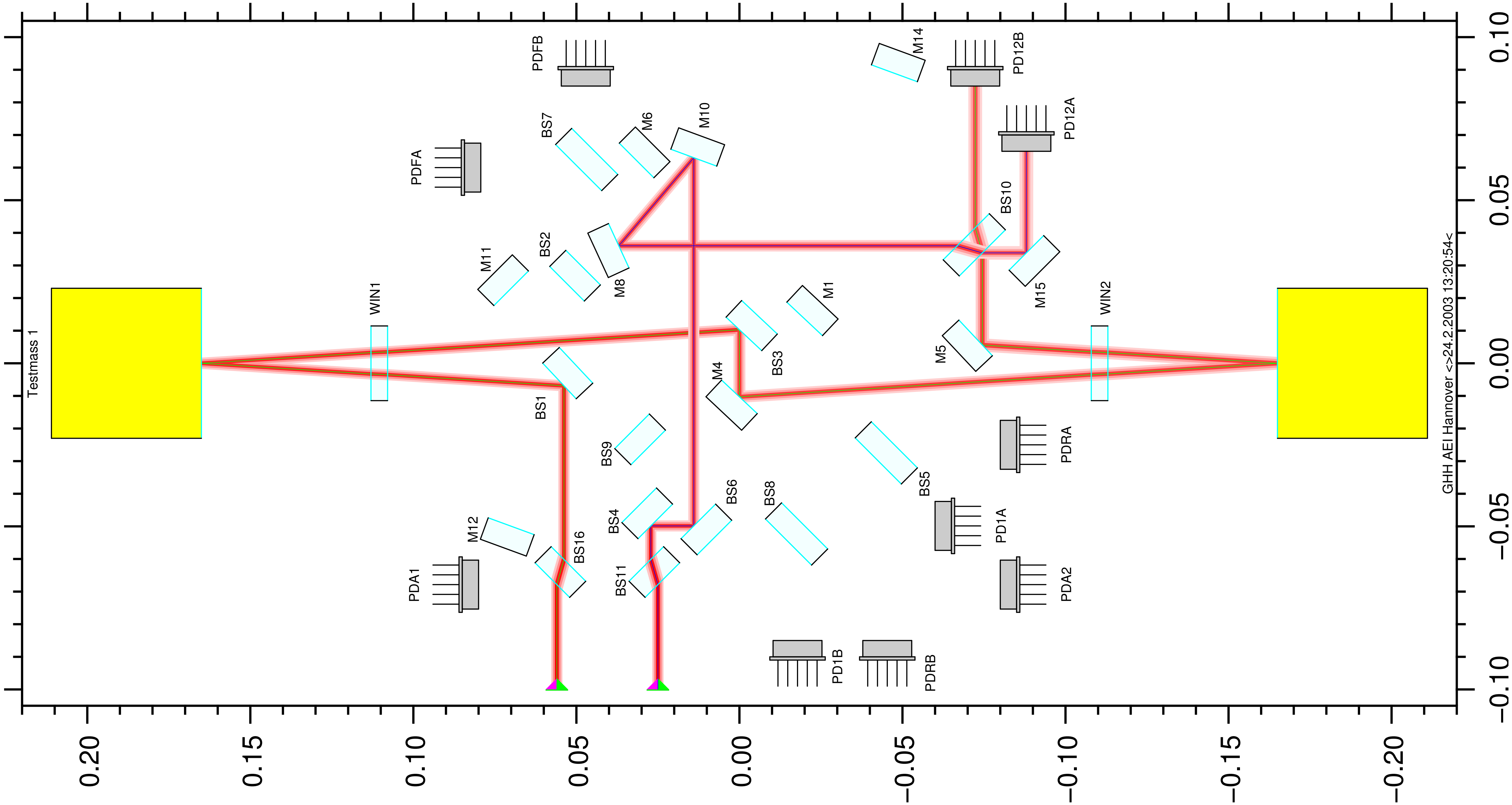

with an extra pathlength of 356.7 mm in the reference fiber, the pathlength difference is 0.000 mm.

x_1

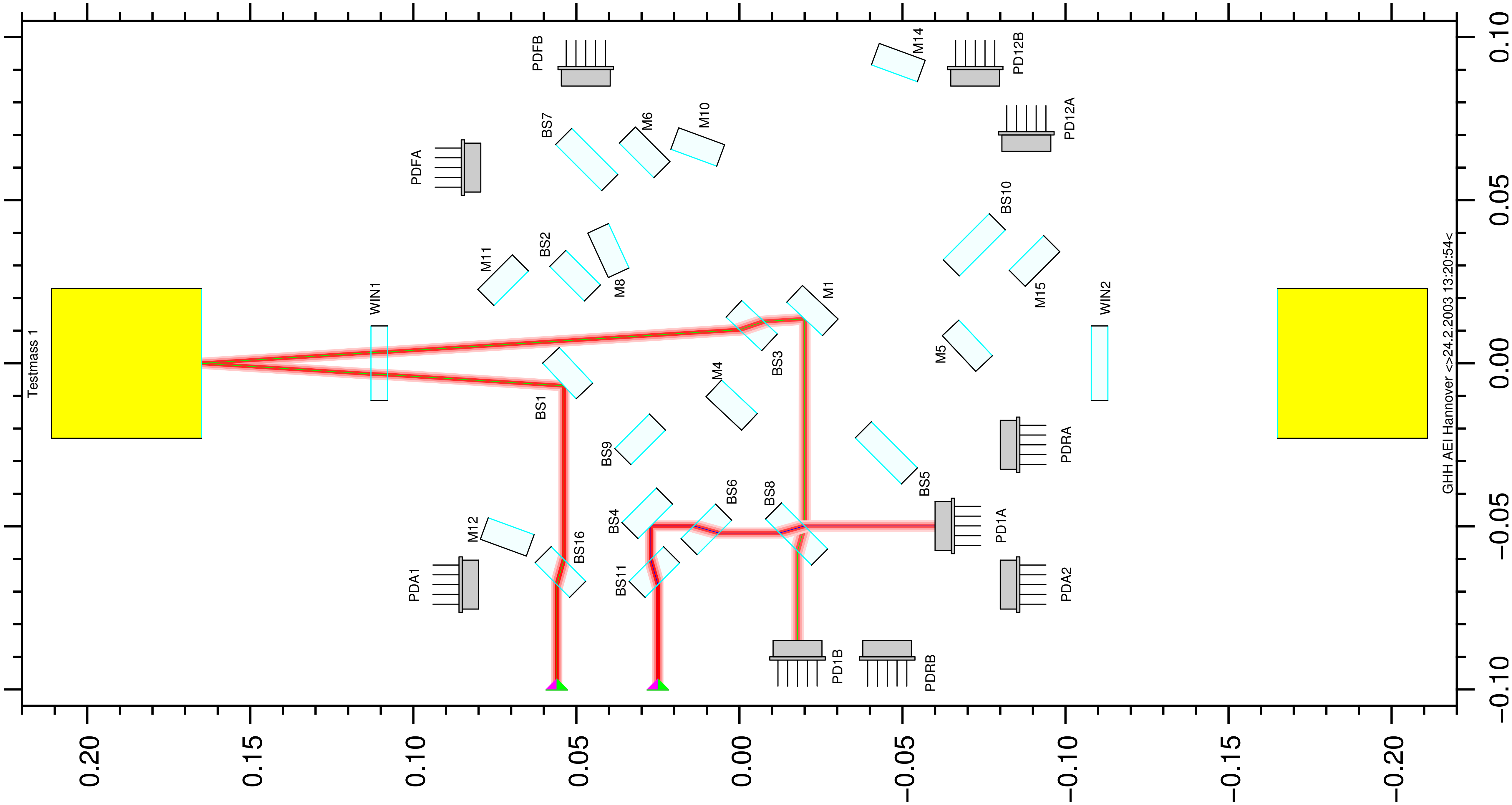

with an extra pathlength of 356.7 mm in the reference fiber, the pathlength difference is 0.02 mm.

Reference

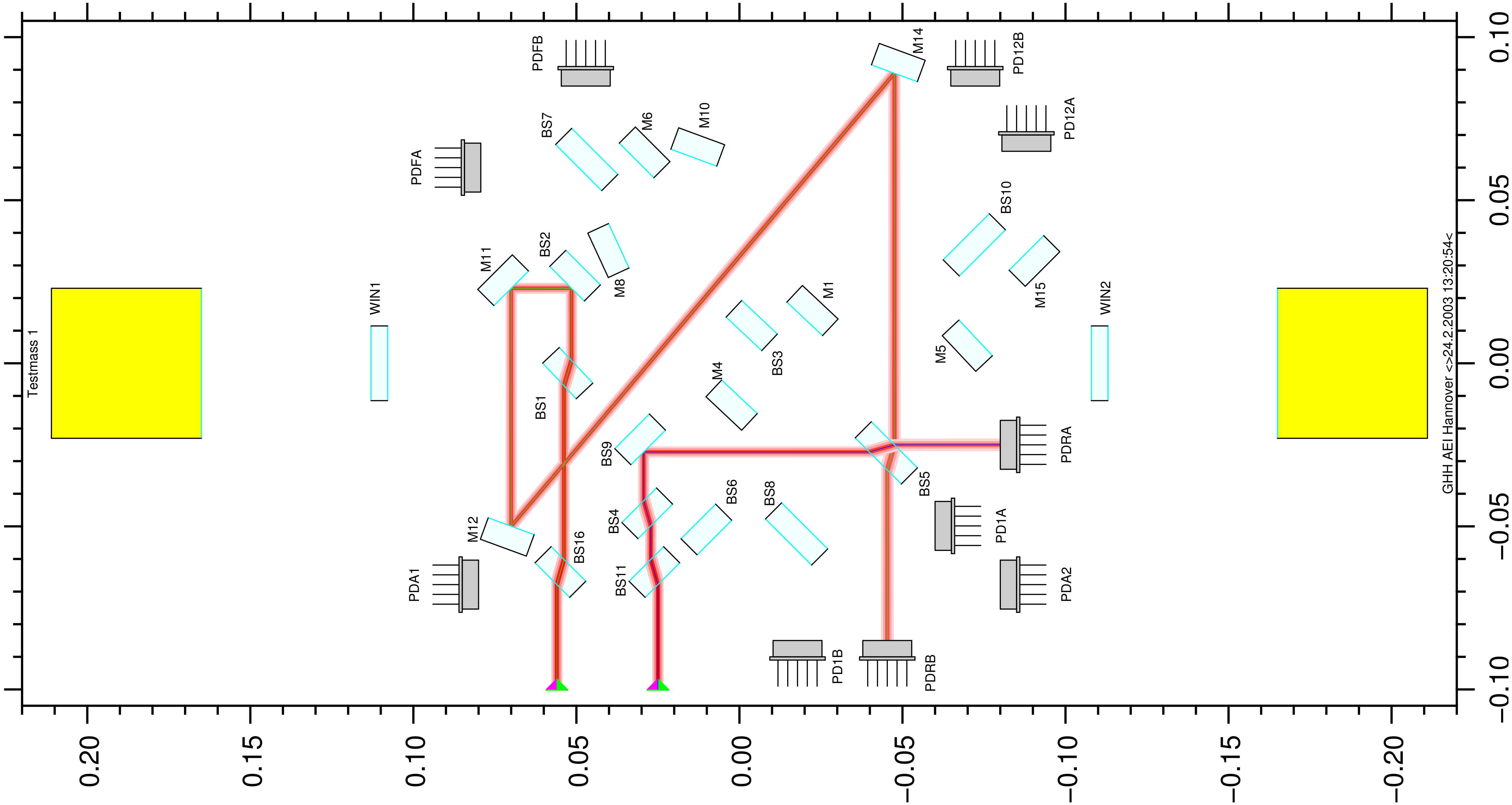

with an extra pathlength of 356.7 mm in the reference fiber, the pathlength difference is 0.016 mm.

Frequency

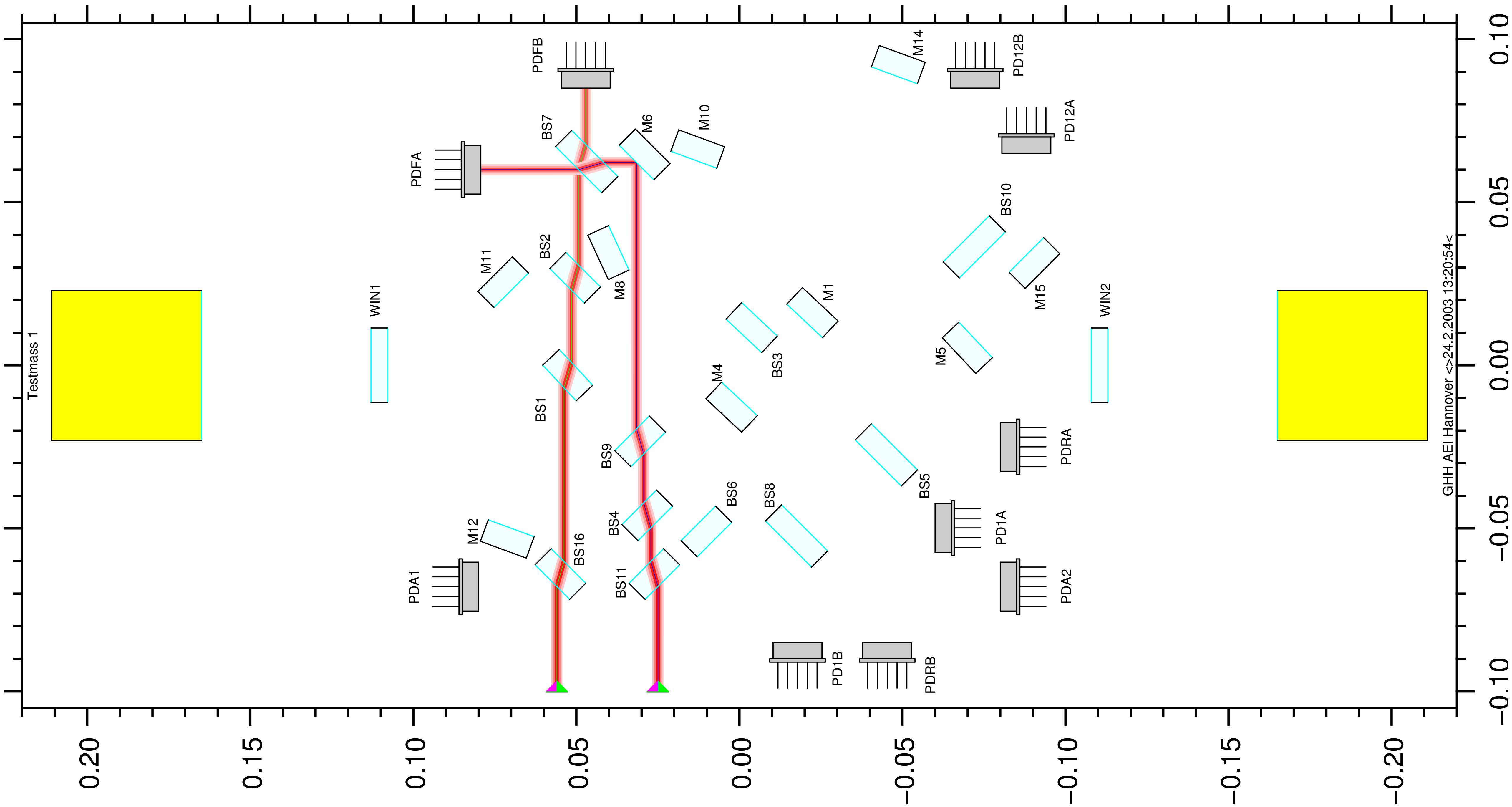

with an extra pathlength of 356.7 mm in the reference fiber, the pathlength difference is −380 mm.

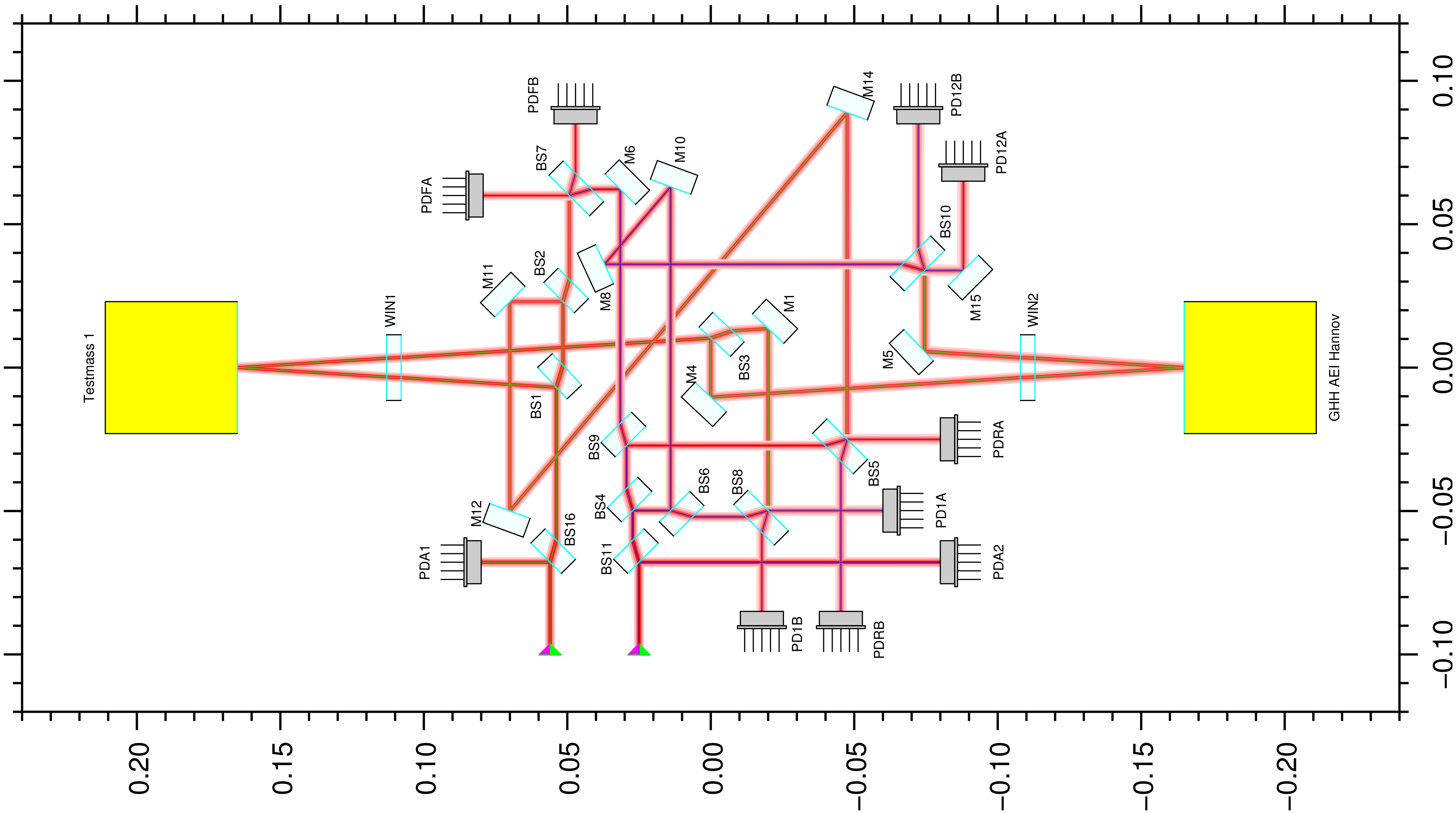

Testmass 1
WIN1
WIN2
GHH AEI Hannov
PDFB
PD12B
PD12A
PDFA
PDA1
PDA2
PDRA
PDRB
PD1A
PD1B
BS1
BS2
BS3
BS4
BS5
BS6
BS7
BS8
BS9
BS10
BS11
BS16
M1
M4
M5
M6
M8
M10
M11
M12
M14
M15
0.20
0.15
0.10
0.05
0.00
−0.05
−0.10
−0.15
−0.20

Optical bench manufacturing

The OB was manufactured by RAL from a Zerodur baseplate and fused silica optical components, using hydroxycatalysis bonding from U Glasgow and the optical design from AEI.

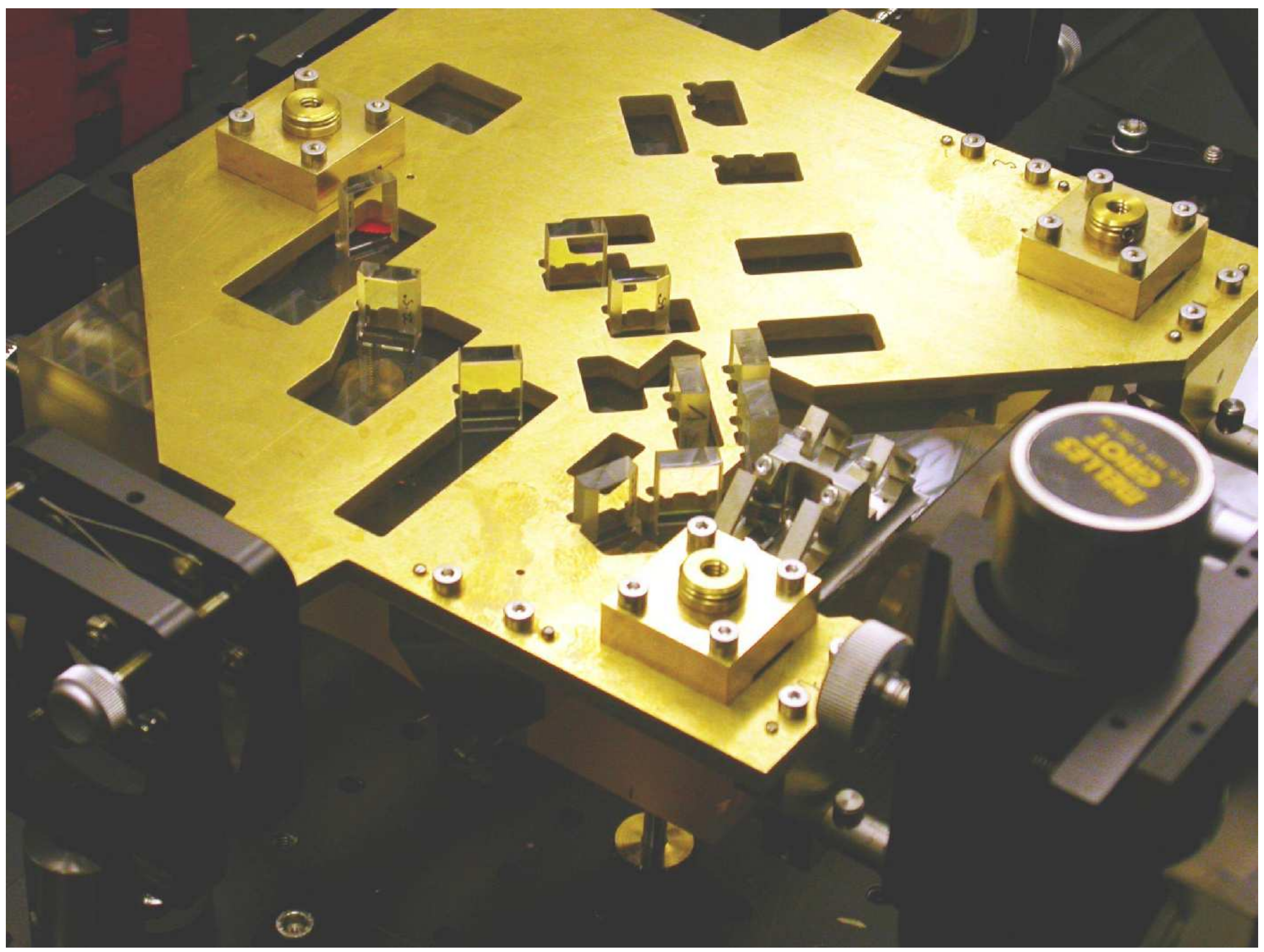

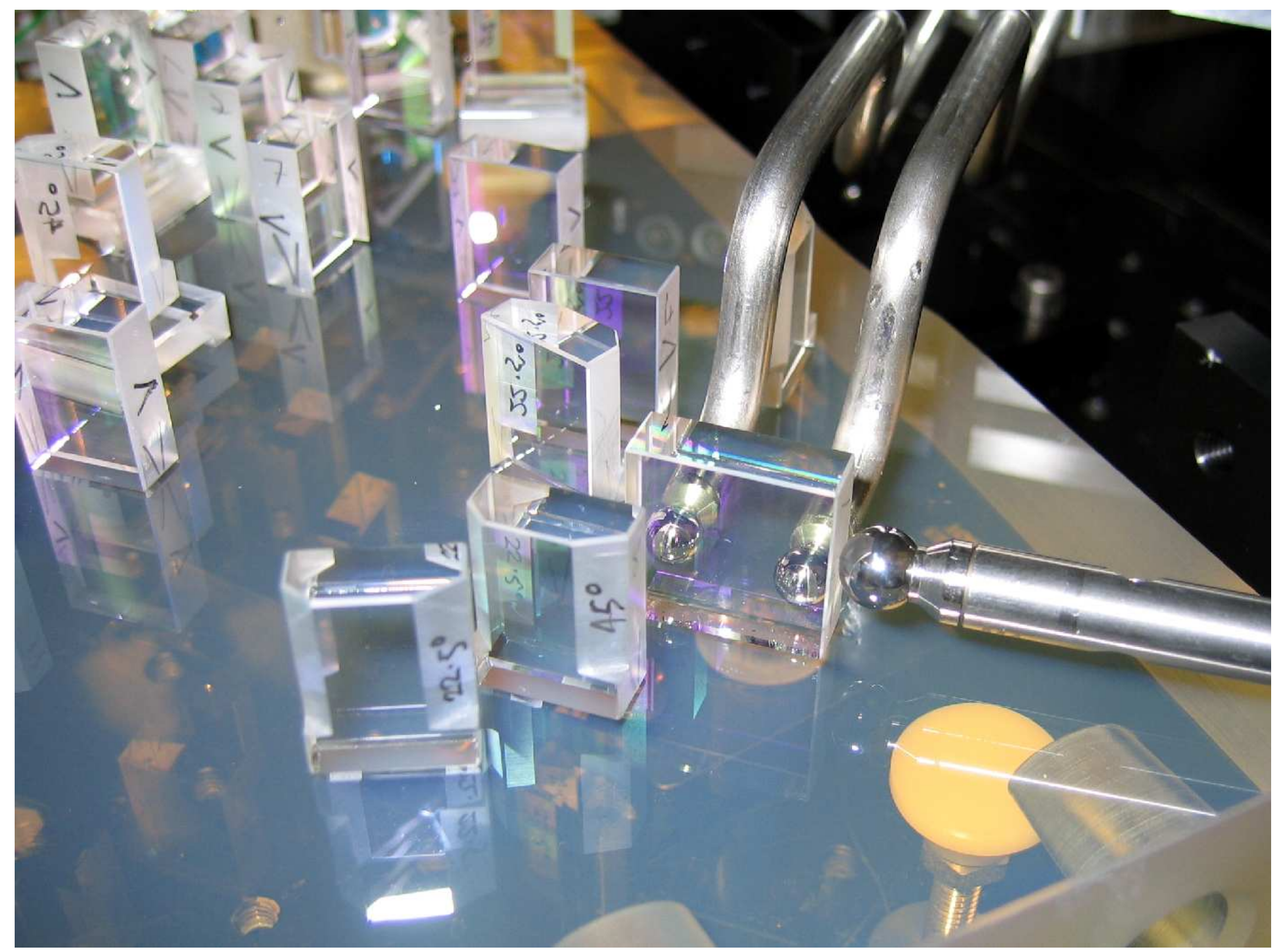

Recovery from accident

A handling mistake caused 4 components to break at a late assembly stage. They could be repaired with interface plates ('bridges').

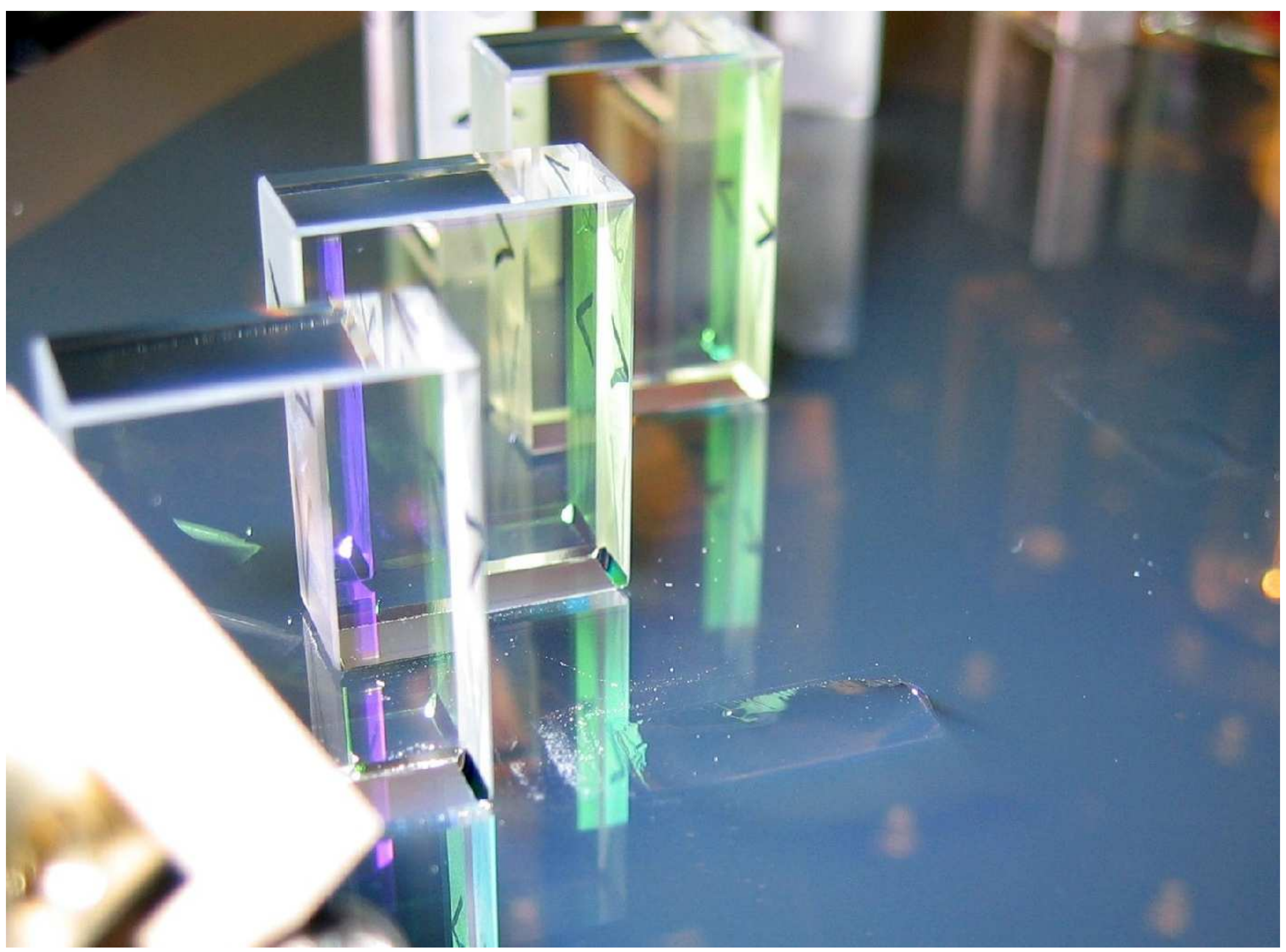

Remaining assembly problems

One bond is incomplete:

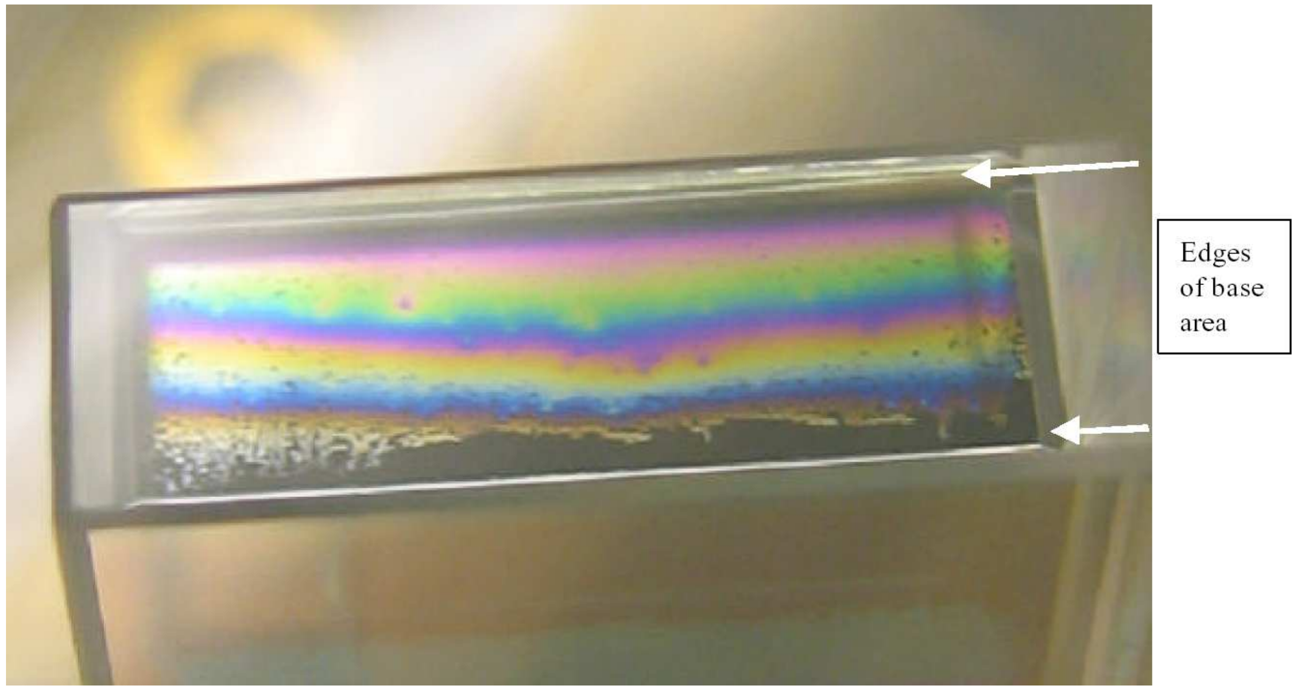

Refinement of the bonding procedure is needed.

The alignment procedure of the fiber injectors needs some refinement ($\approx 100\,\mu$rad vertical error).

More components need to be aligned with the 'jig' (horizontal template accuracy insufficient for long lever arms).

Laser source

The laser (by Tesat) is already space qualified and delivers 25 mW at the end of an optical fiber.

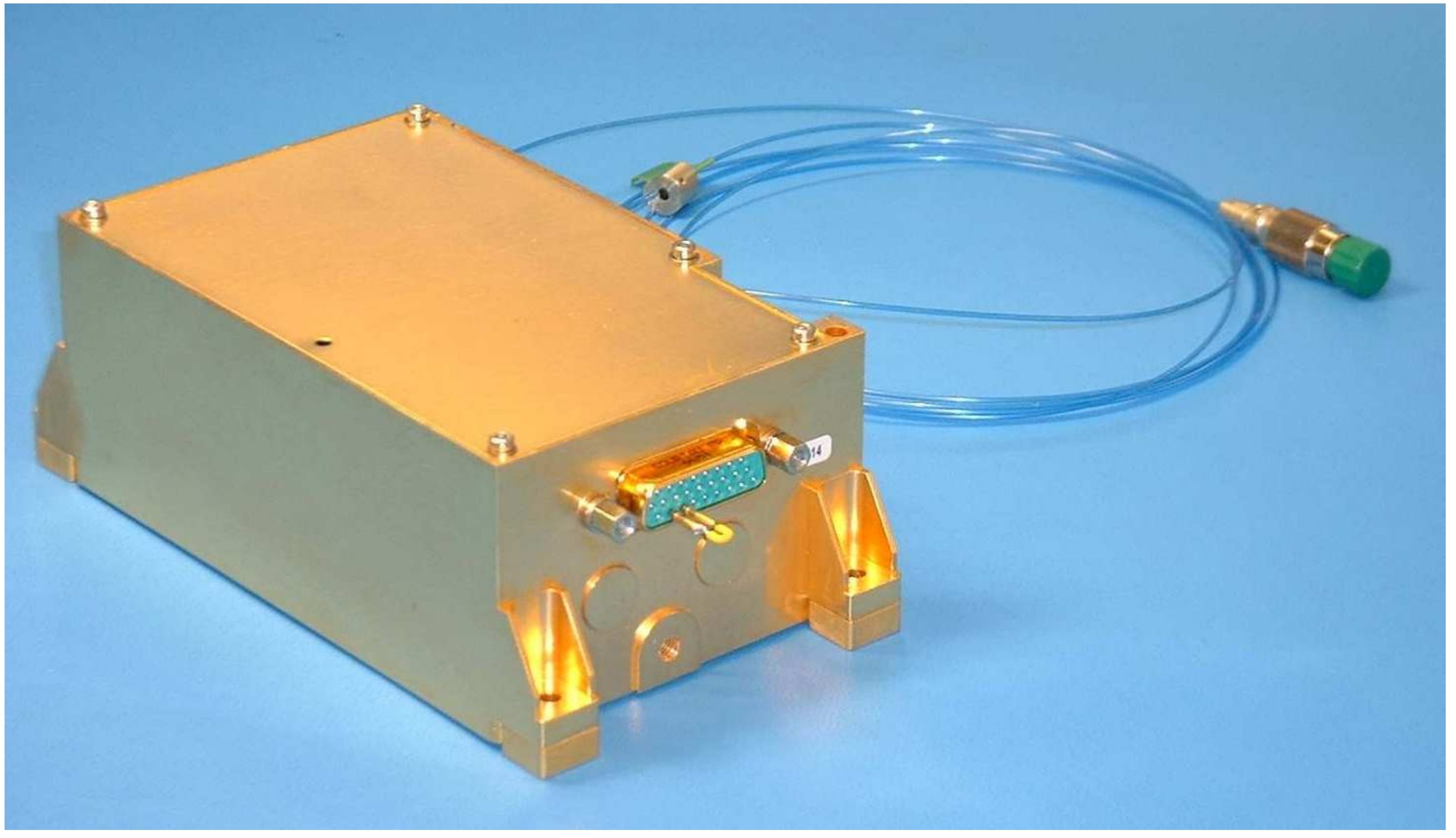

It will be included in a larger box together with the Acousto optical modulators and associated electronics.

AOM Prototype (Contraves)

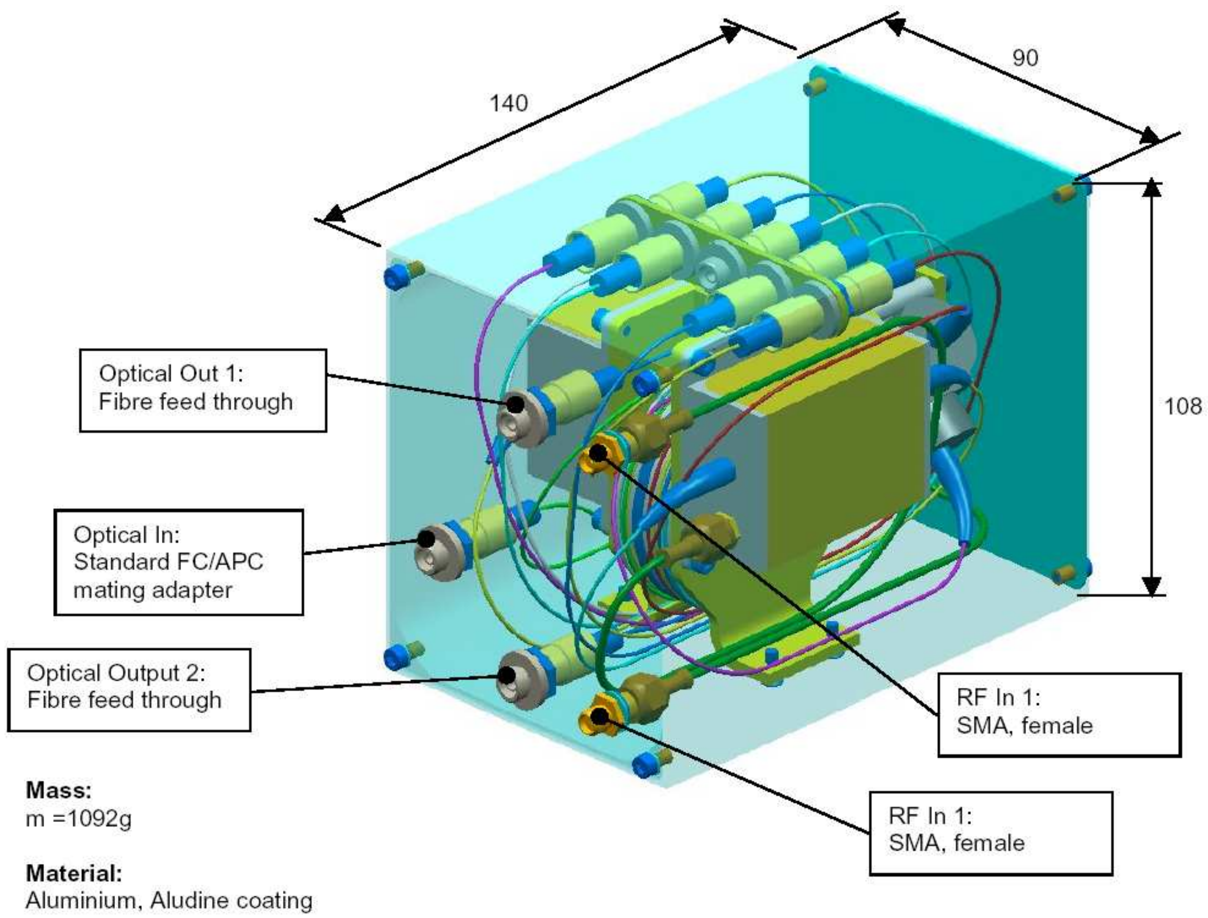

3D-plot of the mechanical layout of the Modulation Bench

Note: The figure shows FC/APC mating adapters for the outputs; To avoid losses these are substituted by fibre feed throughs.

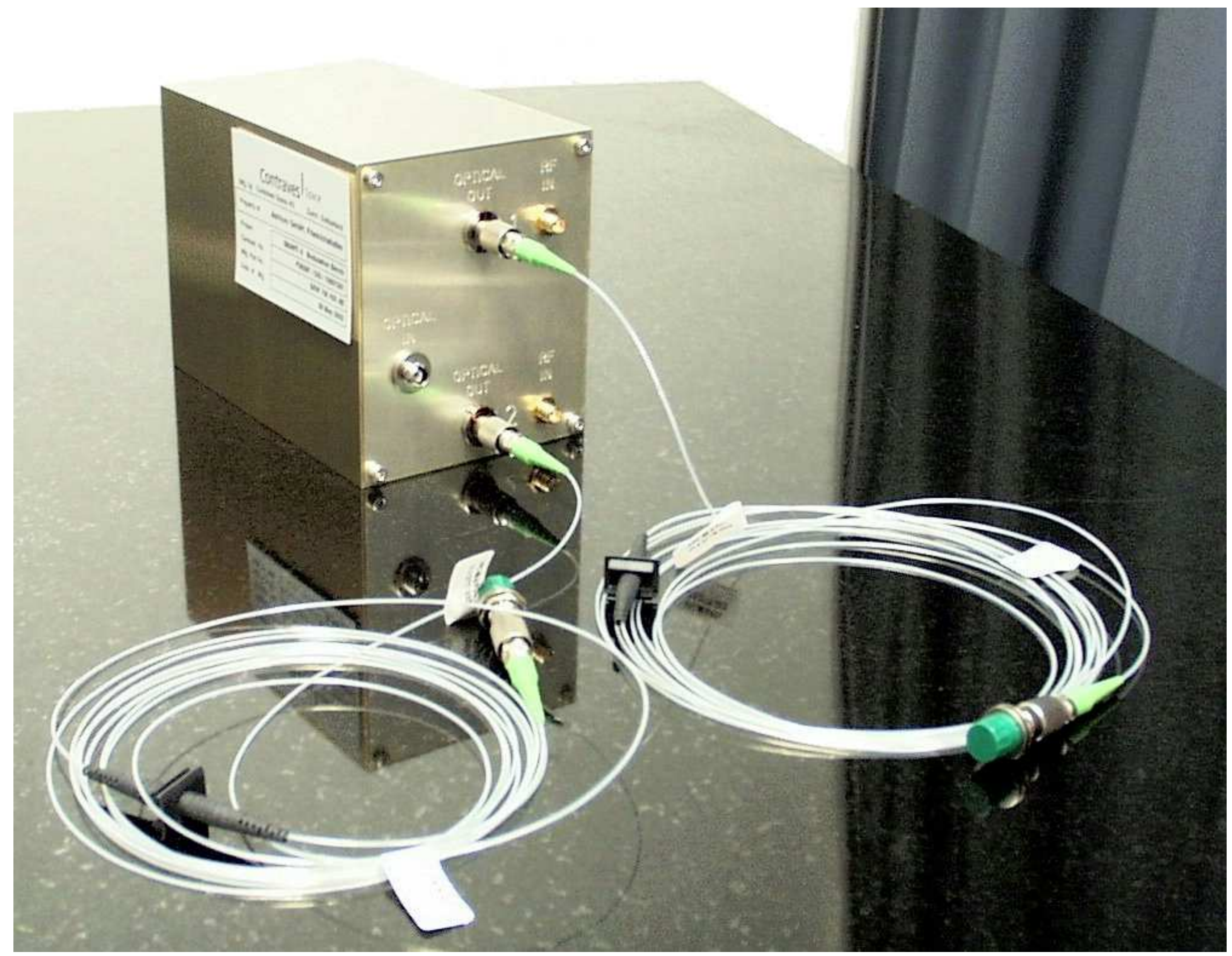

needs further development.

Functional overview

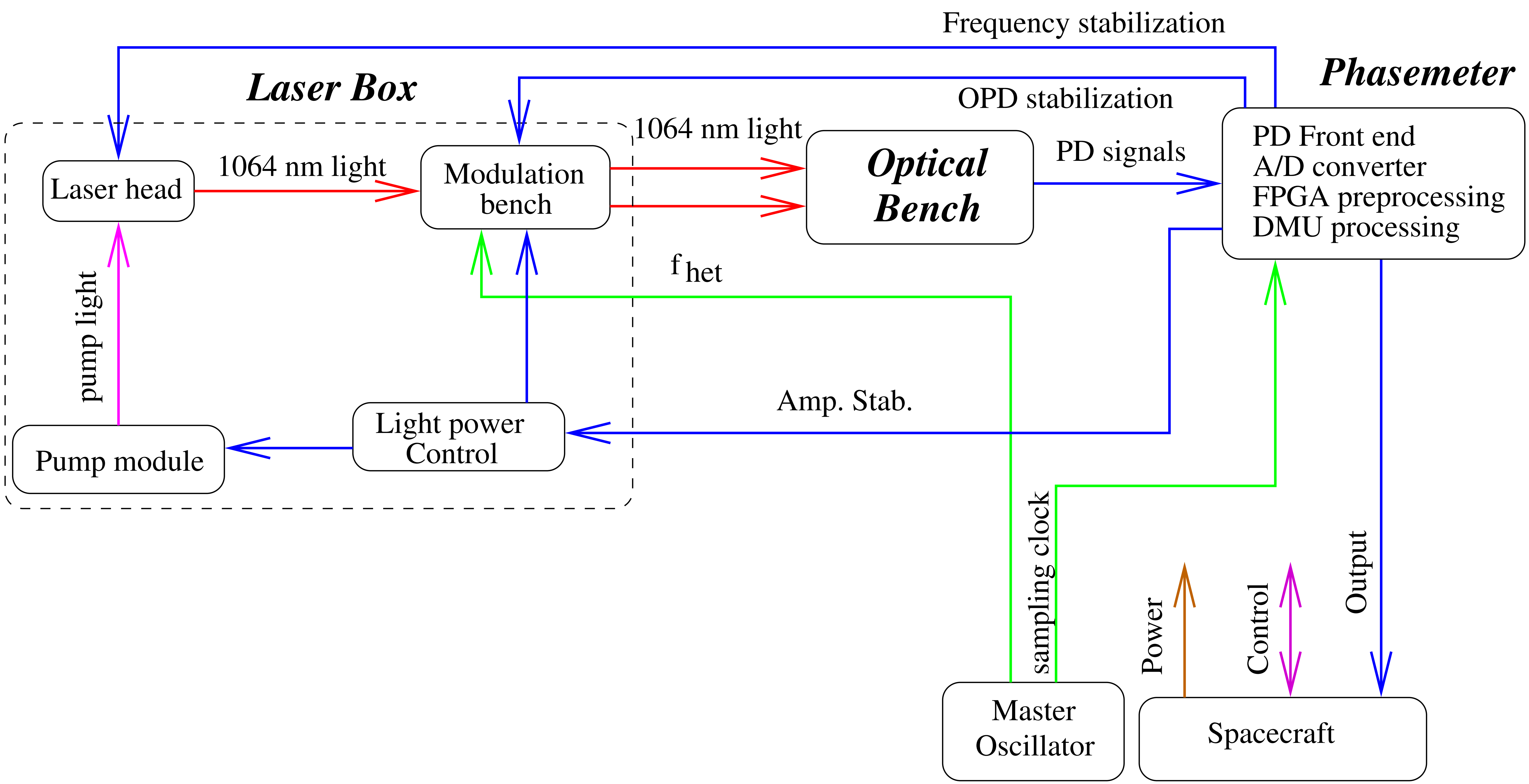

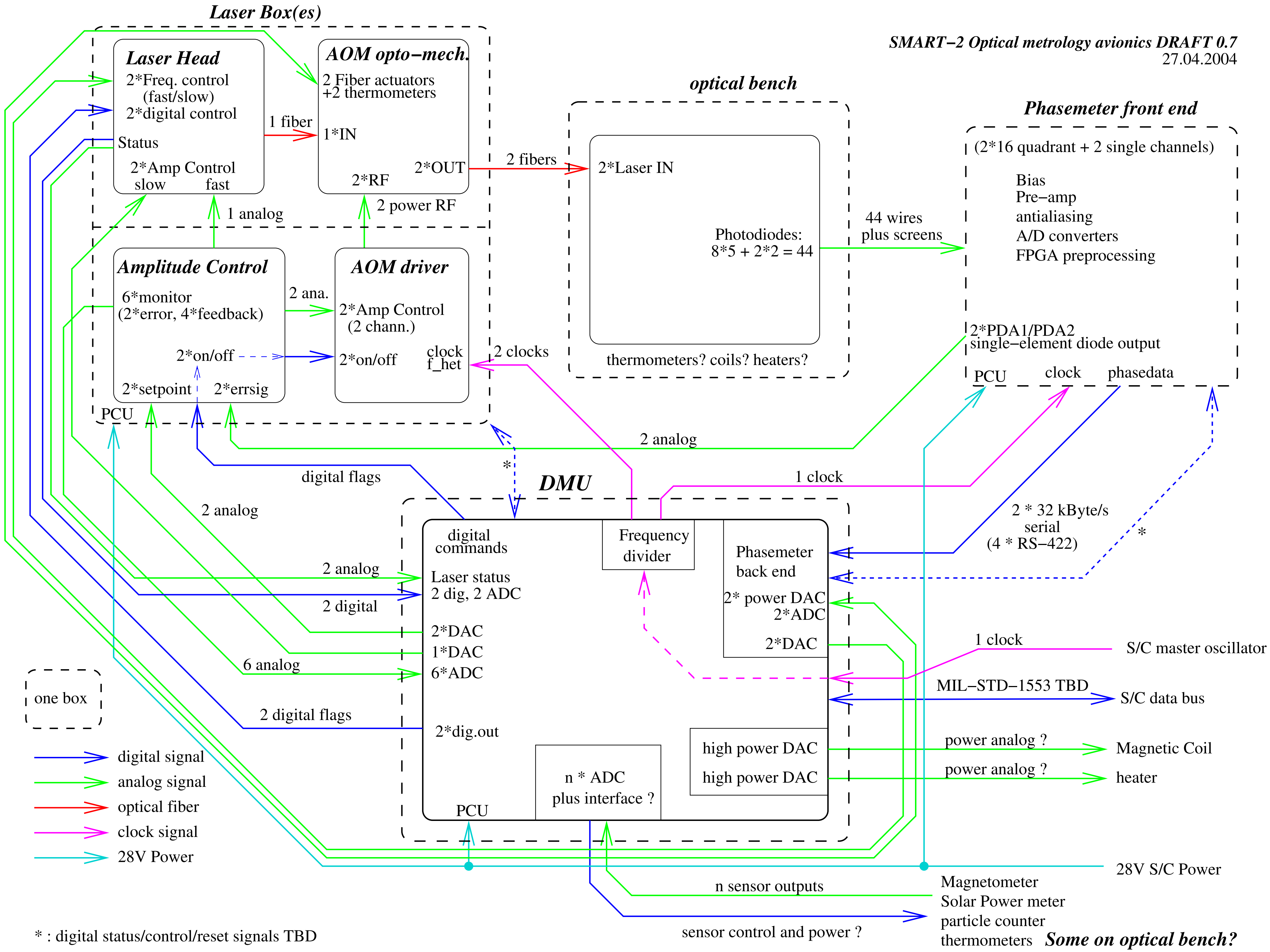

SMART−2 Optical metrology avionics DRAFT 0.7
27.04.2004
Laser Box(es)
Laser Head
2*Freq. control
(fast/slow)
2*digital control
Status
2*Amp Control
slow fast
1 fiber
AOM opto−mech.
2 Fiber actuators
+2 thermometers
1*IN
2*OUT
2*RF
2 fibers
1 analog
2 power RF
Amplitude Control
6*monitor
(2*error, 4*feedback)
2*on/off
2*setpoint
2*errsig
2 ana.
AOM driver
2*Amp Control
(2 chann.)
2*on/off
clock
f_het
2 clocks
PCU
optical bench
2*Laser IN
Photodiodes:
8*5 + 2*2 = 44
thermometers? coils? heaters?
44 wires
plus screens
Phasemeter front end
(2*16 quadrant + 2 single channels)
Bias
Pre−amp
antialiasing
A/D converters
FPGA preprocessing
2*PDA1/PDA2
single−element diode output
PCU
clock
phasedata
2 analog
digital flags
*
DMU
1 clock
2 analog
2 * 32 kByte/s
serial
(4 * RS−422)
*
digital
commands
Frequency
divider
Phasemeter
back end
2 analog
Laser status
2 dig, 2 ADC
2 digital
2* power DAC
2*ADC
2*DAC
2*DAC
1*DAC
6*ADC
6 analog
1 clock
S/C master oscillator
MIL−STD−1553 TBD
S/C data bus
2 digital flags
2*dig.out
high power DAC
high power DAC
power analog ?
Magnetic Coil
power analog ?
heater
n * ADC
plus interface ?
PCU
28V S/C Power
n sensor outputs
Magnetometer
Solar Power meter
particle counter
thermometers
Some on optical bench?
sensor control and power ?
one box
digital signal
analog signal
optical fiber
clock signal
28V Power
* : digital status/control/reset signals TBD

Laser power stabilization

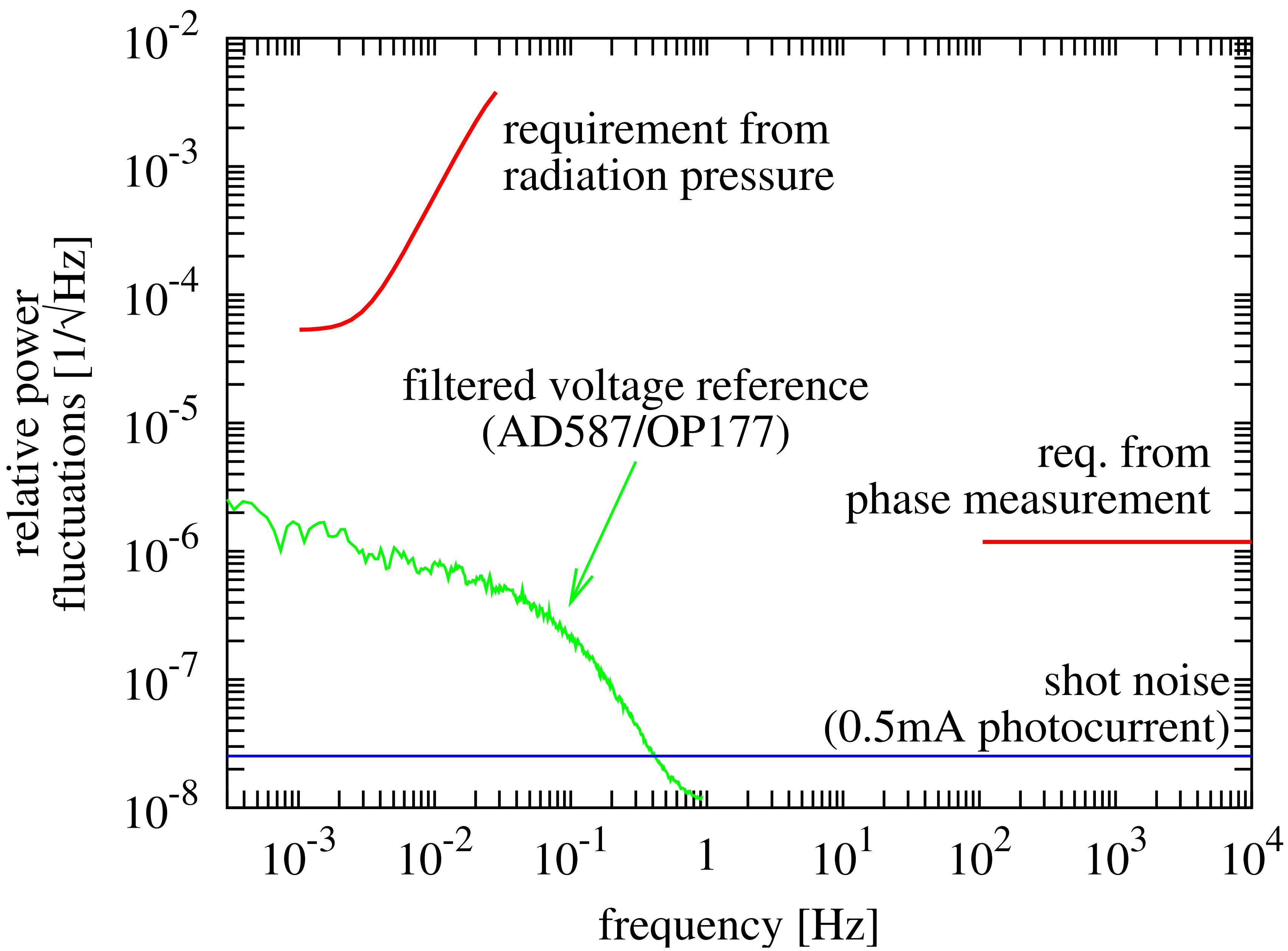

radiation pressure:

$$\frac{\widetilde{\delta P}}{P} < \frac{m\,c\,\omega^2}{2P}\,\widetilde{\delta y} \quad \text{at 1 mHz}$$

phase measurement:

$$\frac{\widetilde{\delta P}}{P} < \frac{c}{2\sqrt{2}}\,\widetilde{\delta \varphi} \quad \text{at } f_{\text{het}}$$

Stabilization via split feedback to Laser pump module (common mode) and AOM RF power (differential mode, BW>50 kHz).

AOM driver

A laboratory prototype of the AOM driver was built and characterized. It consists of two independent TCVCXO's, which are frequency-locked by a PLL to give a constant difference frequency (e.g. 1.6 kHz).

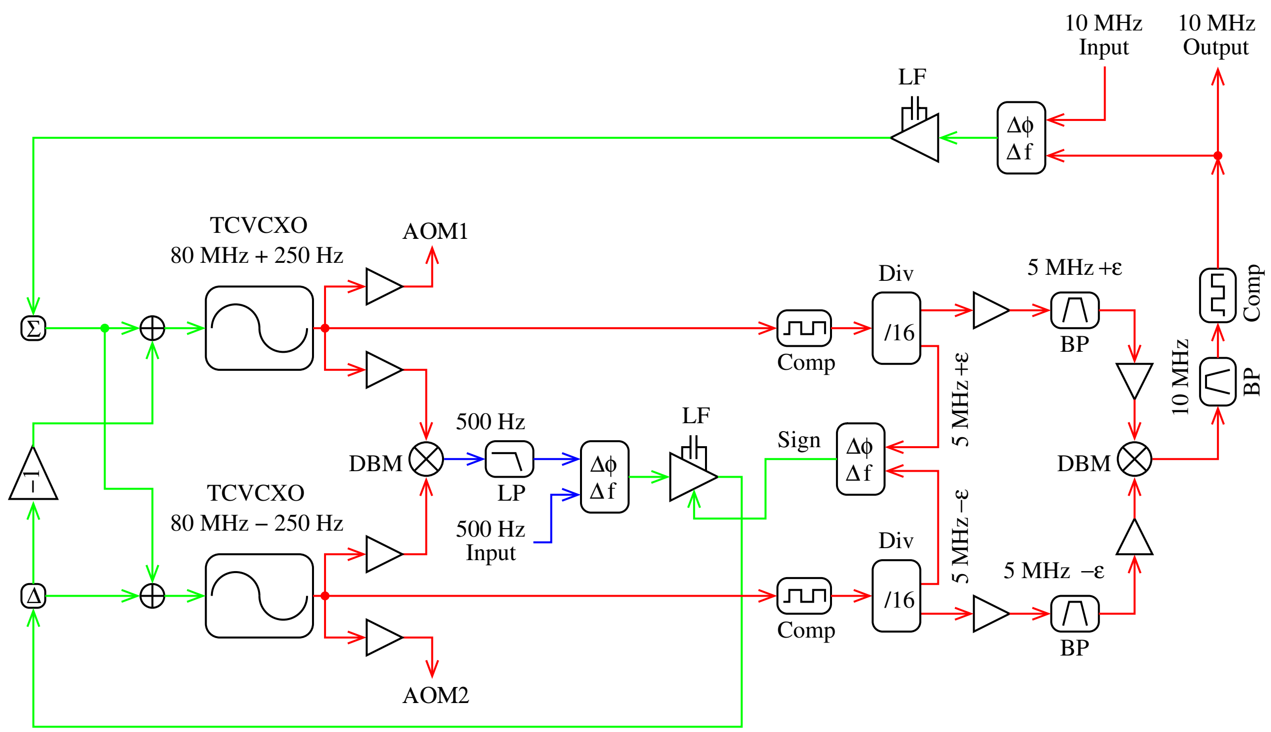

TCVCXO = temperature compensated voltage controlled crystal oscillator
LP = lowpass filter
BP = bandpass filter
LF = loop filter
Comp = comparator to generate logic level signals
Div = digital frequency divider
DBM = double balanced mixer
ΔφΔf = digital phase/frequency detector

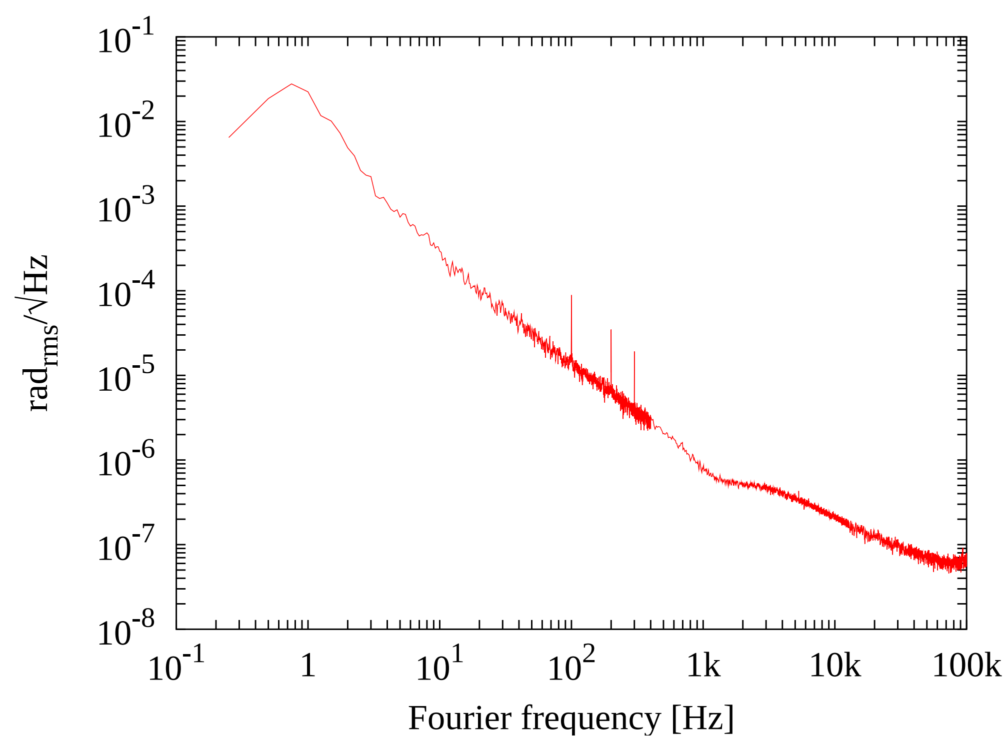

Both the difference frequency ($\approx$ 1.6 kHz) and the average frequency (80 MHz) are controlled by phase-locked loops (PLL).

The phase noise of each oscillator is $< 10^{-6}\,\mathrm{rad}/\sqrt{\mathrm{Hz}}$ at 1 kHz.

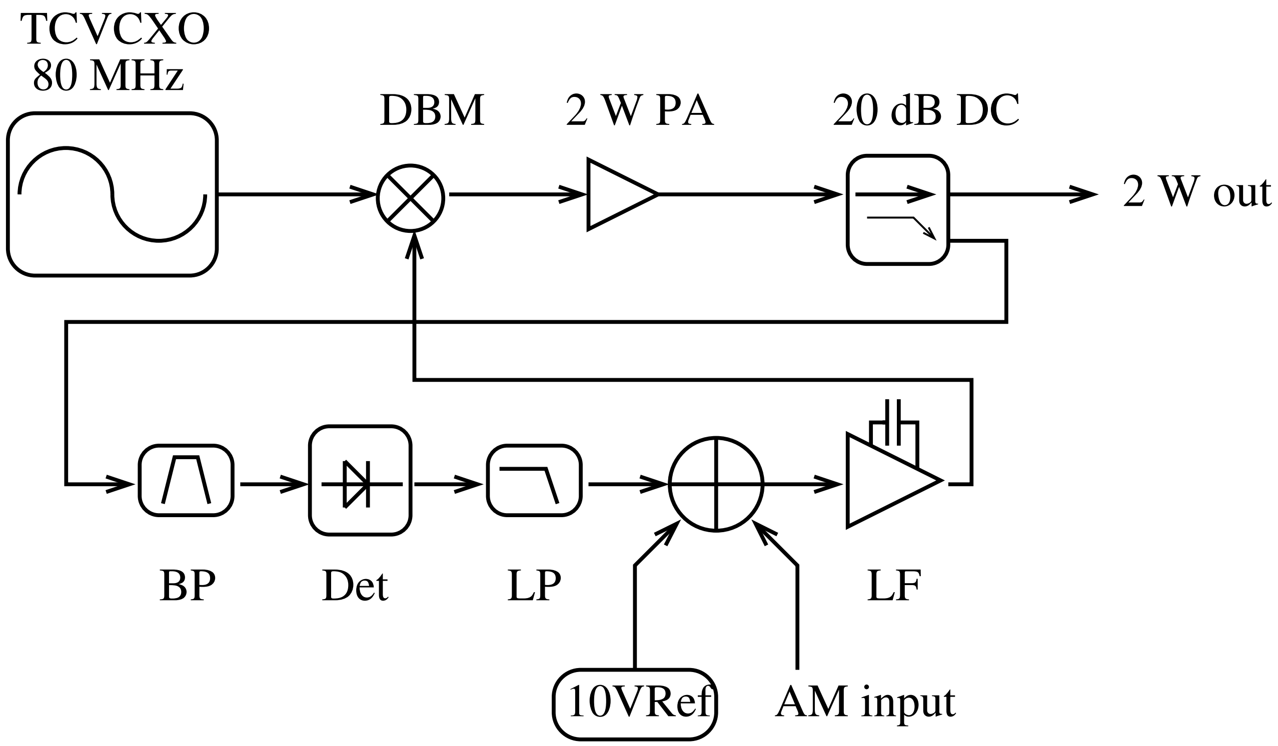

TCVCXO = Temp. compens. VCXO
DBM = double balanced mixer (used as attenuator)
PA = Power Amplifier
DC = Directional Coupler
BP = 80 MHz Bandpass
Det = Schottky Detector
LP = 10 MHz Lowpass
LF = Loop Filter

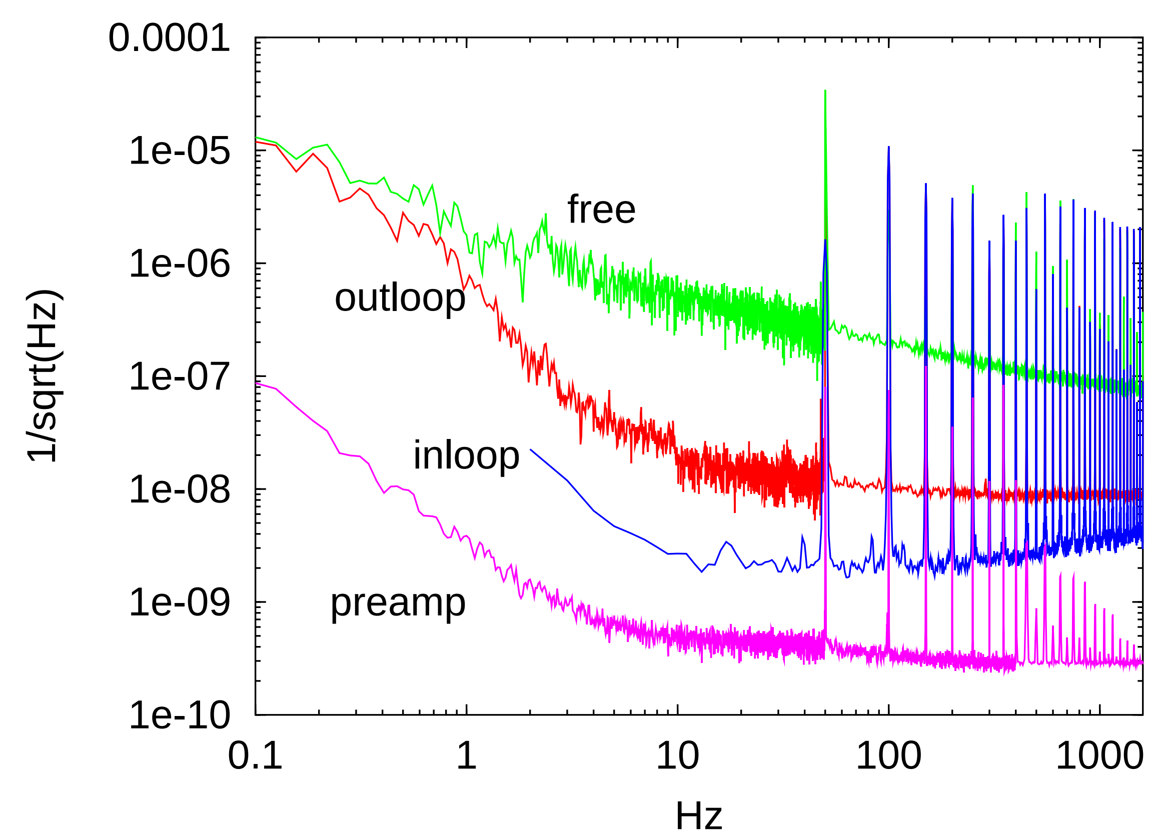

The RF amplitude of each oscillator is stabilized to $\approx 10^{-8}/\sqrt{\text{Hz}}$ at 1 kHz and has a fast input (BW $>$ 100 kHz) to compensate light power fluctuations that are measured at the fiber end.

Laser Frequency noise

Laser frequency fluctuations $\delta\nu = \delta\omega/(2\,\pi)$ cause spurious phase fluctuations $\delta\varphi$ via a **pathlength difference** Δl between the arms.

Conversion factor $\delta\omega$ [rad/s] $\longrightarrow \delta\varphi$:
$\tau = \Delta l/c$, the differential time delay.

Budget: $\delta\varphi < 6\,\mu\text{rad}/\sqrt{\text{Hz}}$
between 3 mHz and 30 mHz

Frequency stability requirement:

$$\widetilde{\delta\nu} = \frac{c}{2\pi\,\Delta l}\,\widetilde{\delta\varphi} = 28\,\frac{\text{kHz}}{\sqrt{\text{Hz}}}\Big/\left[\frac{\Delta l}{1\,\text{cm}}\right]$$

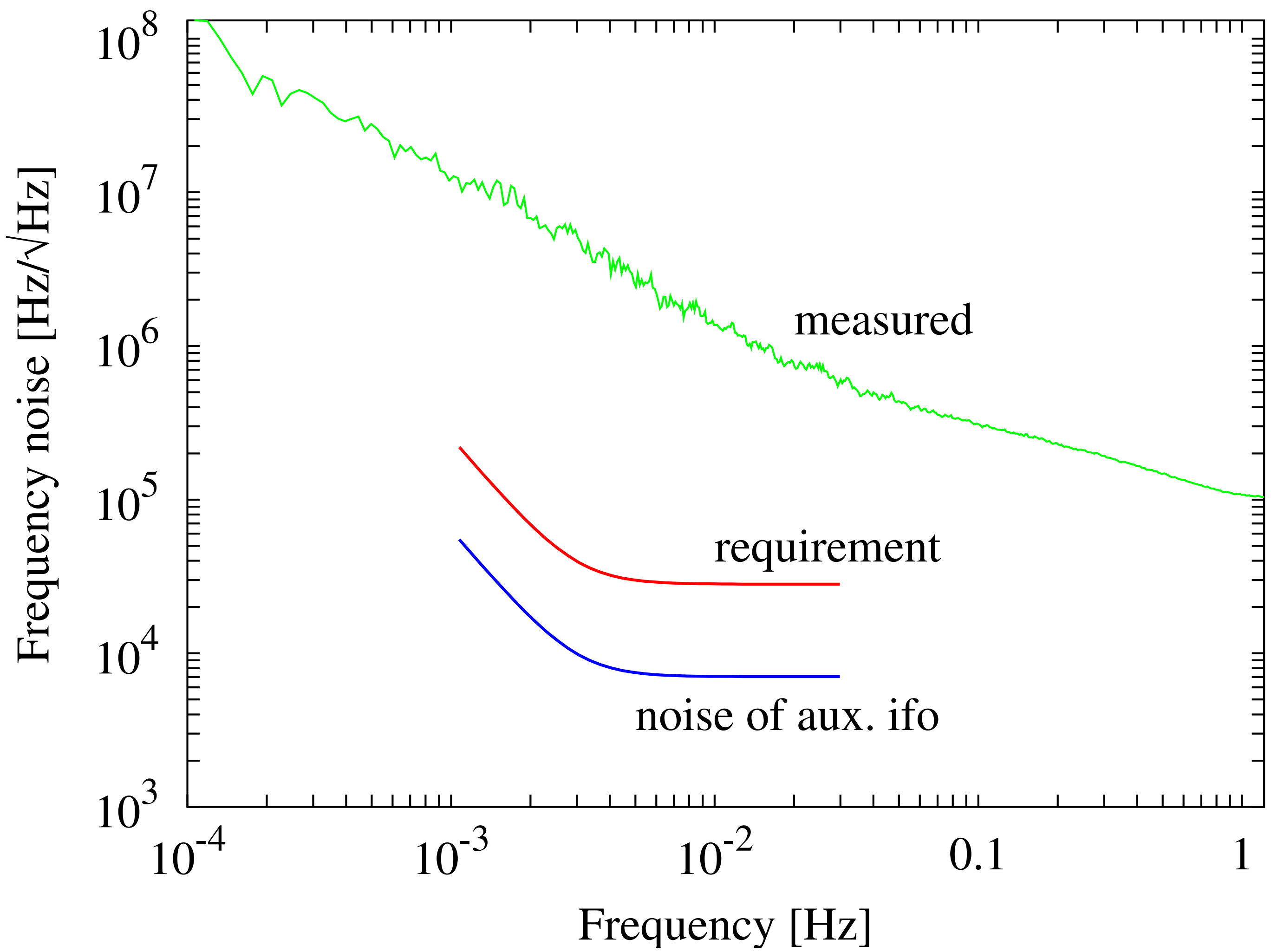

Frequency stabilization

We use the extra interferometer with $\Delta L = 38\,\mathrm{cm}$ as sensor with sufficiently low noise. Two options are:

- Use that signal in a **feedback loop to actively stabilize** the laser **(the baseline)**:

  Required loop gain : ≈ 100 at $30\,\mathrm{mHz}$.

  With a $1/f$ simple integrator as loop filter we need unity gain frequency $> 3\,\mathrm{Hz}$.

  Allowing an extra phase delay of 45° in the loop gain at $3\,\mathrm{Hz}$, the permissible processing time delay is $40\,\mathrm{ms}$ (achievable).

  Small complication with DC feedback: laser is forced to follow drifts of auxiliary interferometer (solvable).

- Do not stabilize the laser but use that signal to **correct the main output signals** for the frequency flucuations thus measured **(fallback option)**. The actual pathlength differences Δl must be known to relatively high precision: $\delta l = 0.1\,\mathrm{mm}$ and $\delta L = 4\,\mathrm{mm}$. Manufacturing to such accuracy is difficult, but measurement during operation is possible.

Phasemeter using SBDFT (Single-Bin Discrete Fourier Transform)

Inputs from one quadrant diode: $x_i = U_A(t_i)$, same for $U_B(t), U_C(t), U_D(t)$.
First step: **SBDFT** achieves data reduction by a factor of ≈ 100:

$$\text{DC components:} \quad \mathrm{DC}_A, \mathrm{DC}_B, \mathrm{DC}_C, \mathrm{DC}_D \quad \text{(real)}: \quad \mathrm{DC}_A = \sum_{i=0}^{n-1} x_i,$$

$$f_{\text{het}}\,\text{components:} \quad \mathrm{F}_A, \mathrm{F}_B, \mathrm{F}_C, \mathrm{F}_D: \quad \Re(\mathrm{F}_A) = \sum_{i=0}^{n-1} x_i \cdot c_i, \quad \Im(\mathrm{F}_A) = \sum_{i=0}^{n-1} x_i \cdot s_i.$$

The constants s_i and c_i are pre-computed: $c_i = \cos\left(\frac{2\pi\, i\, k}{n}\right), s_i = \sin\left(\frac{2\pi\, i\, k}{n}\right)$.

At the moment, our prototype uses PC software. Prototypes close to the LTP phasemeter (using FPGAs for this step) are under construction in Hannover and Birmingham:

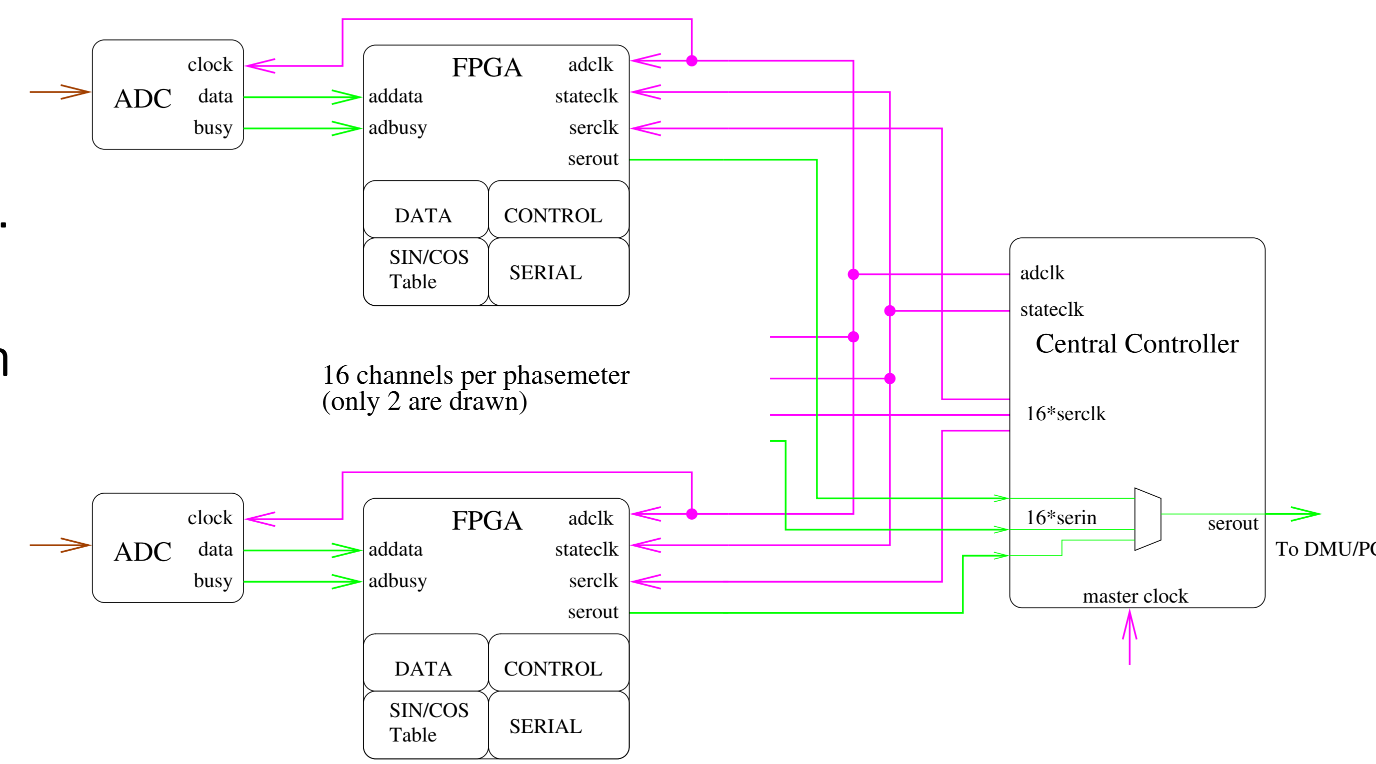

Phasemeter EM/FM concept

– for redundancy, there are 2 separate phasemeters, each processing 4 photodiodes (one from each interferometer) = 16 channels.

– Data rate from ADC: 100 kHz $\times$ 16 bit $\times$ 16 channels = 3.2 MByte/sec.

– Early concepts needed high-speed DSP for DFT.

– **New concept**: Initial data processing stage (SBDFT) is done in hardware (FPGA).
Reduced data rate 100 Hz $\times$ 20 bytes $\times$ 16 channels = 32 kByte/sec, i.e. data reduction by factor 100.
FPGA also handles ADC timing and control.

– DSP is still needed for final processing stages, but with 1/100 of the data rate and no critical timing any more.

– FPGAs exist in rad-tolerant and rad-hard versions, e.g. by Actel.

– Prototype FPGA phasemeters are under construction in Birmingham and Hannover.

Further processing in DMU

Longitudinal Signal:
$\mathsf{F}_{\Sigma}^{(1)} = \mathsf{F}_A + \mathsf{F}_B + \mathsf{F}_C + \mathsf{F}_D$ the total f_{het} amplitude on the first quadrant diode, and
$\mathsf{F}_{\Sigma}^{(2)}$ for the second (reference) quadrant diode equivalently.
$\varphi_{\text{long}} = \arg(\mathsf{F}_{\Sigma}^{(1)}) - \arg(\mathsf{F}_{\Sigma}^{(2)}) + n \cdot 2\pi$, (integer n from phasetracking algorithm).

Alignment signals, independently on each diode:
$\mathsf{F}_{\text{Left}} = \mathsf{F}_A + \mathsf{F}_D$: amplitude in left half, $\mathsf{DC}_{\text{Left}} = \mathsf{DC}_A + \mathsf{DC}_D$: average in left half,
$\mathsf{F}_{\text{Right}}$, $\mathsf{F}_{\text{Upper}}$, $\mathsf{F}_{\text{Lower}}$, $\mathsf{DC}_{\text{Right}}$, $\mathsf{DC}_{\text{Upper}}$, $\mathsf{DC}_{\text{Lower}}$ equivalently.

The DC (center of gravity) signals:

$$\Delta x = \frac{\mathsf{DC}_{\text{Left}} - \mathsf{DC}_{\text{Right}}}{\mathsf{DC}_{\Sigma}}, \quad \Delta y = \frac{\mathsf{DC}_{\text{Upper}} - \mathsf{DC}_{\text{Lower}}}{\mathsf{DC}_{\Sigma}},$$

The DWS (differential wavefront sensing) signals:

$$\Phi_x = \arg\left(\frac{\mathsf{F}_{\text{Left}}}{\mathsf{F}_{\text{Right}}}\right), \quad \Phi_y = \arg\left(\frac{\mathsf{F}_{\text{Upper}}}{\mathsf{F}_{\text{Lower}}}\right),$$

Alignment signals are obtained from each quadrant diode individually (no reference needed)
$\longrightarrow$ Rejection of several common mode noise sources.

Optical windows

There will be 4 transmissions through an optical window of approx. 5 mm thickness in the main $x_1 - x_2$ measurement path:

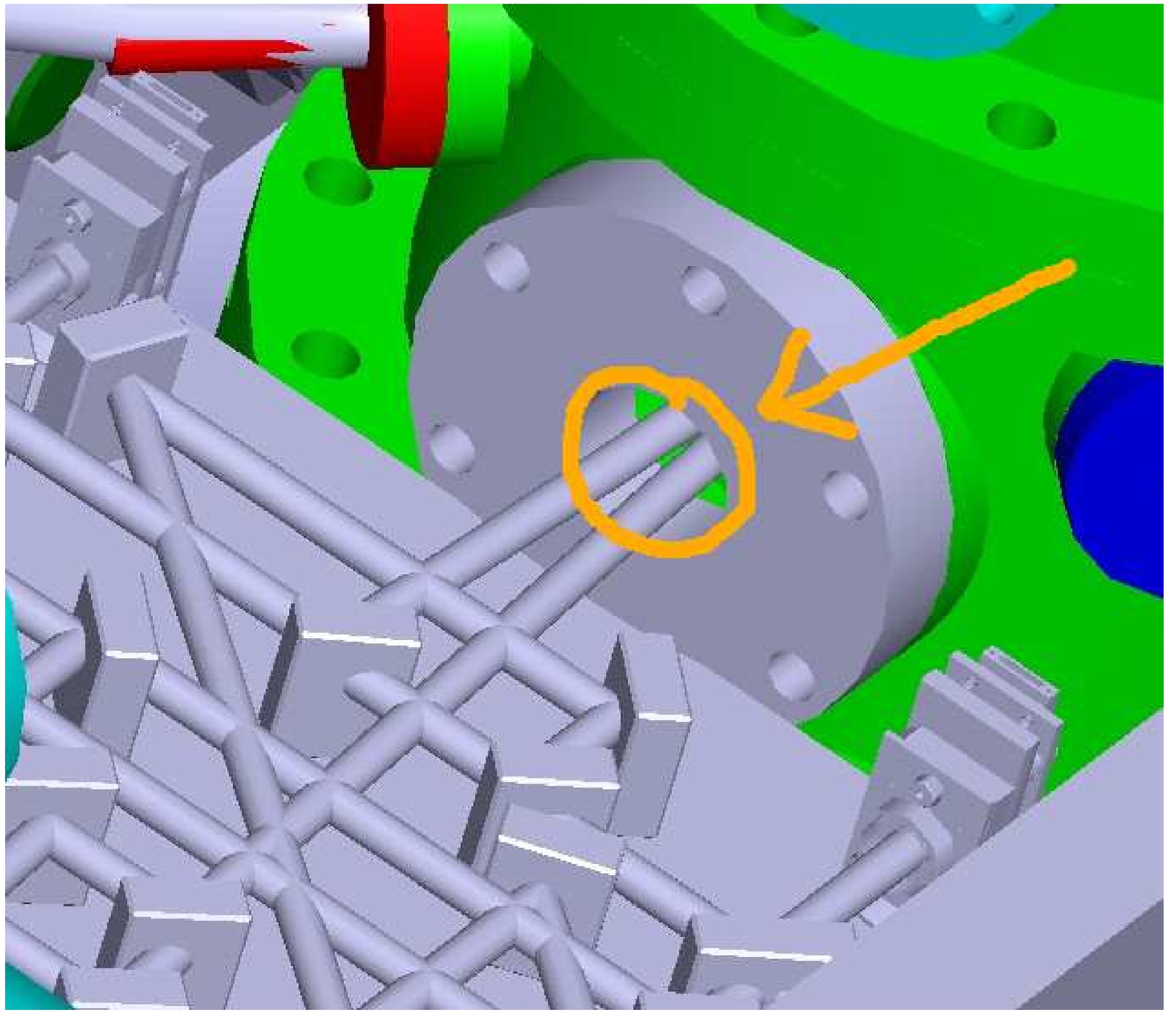

Pathlength effects

Four major disturbing effects on the optical pathlength are expected:

Thermal variation of optical pathlength.

Stress-induced change in refractive index.

mechanical motion of the window in z-direction.

mechanical tilt fluctuations of the window.

The sum of all noise contributions of one window (in double pass) is counted as one interferometer noise source and allocated a bufget of $1\,\mathrm{pm}/\sqrt{\mathrm{Hz}}$. Hence the window effects contribute no more than $1\,\mathrm{pm}/\sqrt{\mathrm{Hz}}$ in the x_1 measurement and no more than $2\,\mathrm{pm}/\sqrt{\mathrm{Hz}}$ in the $x_1 - x_2$ measurement. Each effect is allocated $0.33\,\mathrm{pm}/\sqrt{\mathrm{Hz}}$ (for one window double pass).

Thermal variation of optical pathlength:

$\Delta s = \Delta T \times L \times \left(\frac{\mathrm{d}n}{\mathrm{d}T} + (n-1)\alpha\right).$

$\mathrm{d}n/\mathrm{d}T + (n-1)\alpha$ is ≈ 5 ppm/K for most glasses (e.g. BK7).

Athermal glasses (e.g. Ohara S-PHM52, Schott N-FK51 and Schott N-FK56) have $\underline{0.5 \ldots 1\,\mathrm{ppm/K}}$.

The Schott glasses have a high $\alpha \approx 15$ppm/K, not well matched to Ti.

The best candidate that we identifed so far is Ohara S-PHM52.

At 1064 nm, $\mathrm{d}n/\mathrm{d}T + (n-1)\alpha = 0.59$ ppm/K.

The linear thermal expansion coefficient α is 10.1 ppm/K, well matched to Ti.

All these athermal glasses are difficult to polish and very **brittle**, which may limit the mounting options. With glueing, care must be taken to avoid high static stresses that might cause the glass to break in thermal cycling.

From $\widetilde{\delta T} = \frac{\widetilde{\delta s}}{L \times \left(\frac{\mathrm{d}n}{\mathrm{d}T} + (n-1)\alpha\right)}$,
a pathlength error of $\widetilde{\delta s} = 0.33\,\mathrm{pm}/\sqrt{\mathrm{Hz}}$
and $L = 12\,\mathrm{mm}$,
the required thermal stability at the window is:
$\widetilde{\delta T} < 4 \cdot 10^{-5}\,\mathrm{K}/\sqrt{\mathrm{Hz}}$

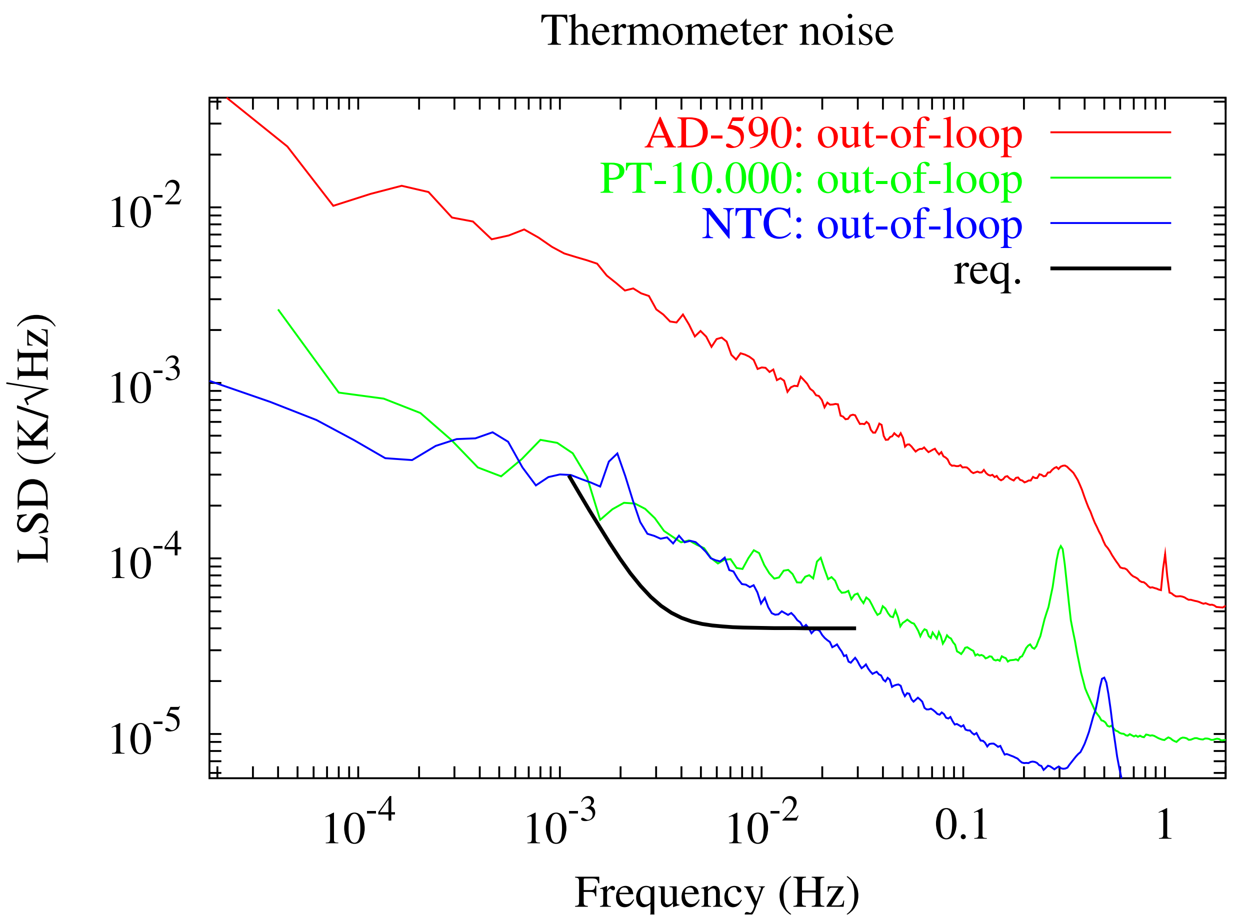

<u>Ohara S-PHM52</u>
Linear thermal expansion $\alpha = 10.1$ppm/K.

at 1064 nm:

$n = 1.60645$,

$\mathrm{d}n/\mathrm{d}T + (n-1)\alpha = 0.589\,\mathrm{ppm/K}$.

Stress-induced change in refractive index:

While in some materials the stress-induced **birefringence** can be made small, we have here the absolute variation in refractive index, which is never small. The relevant material constant is:

"Photoelastic constant" $\beta = 1.0\,\mathrm{nm/cm}/10^5\mathrm{Pa}$.

For a pathlength error of $0.33\,\mathrm{pm}/\sqrt{\mathrm{Hz}}$ and $L = 12\,\mathrm{mm}$, the required stability of mechanical stress in the window is:

$$\widetilde{\delta\sigma} < 30\,\mathrm{Pa}/\sqrt{\mathrm{Hz}}.$$

We have no knowledge of the real stress fluctuation.
This error might be big.
Mounting of the optical window will be critical (In seal? Au-Sn seal?).
Measuring the thermally induced pathlength fluctuation is essential.

Mechanical motion:

If there is a deviation γ from parallelism and the window moves in z direction by Δz this yields a pathlength error (double-pass):

$$\Delta s = 2\gamma(n-1)\Delta z.$$

For $\gamma = 30''$, $n-1 = 0.6$ and a pathlength error of $0.33\,\mathrm{pm}/\sqrt{\mathrm{Hz}}$ one gets

$$\widetilde{\delta z} < 2\,\mathrm{nm}/\sqrt{\mathrm{Hz}}.$$

If this is difficult, the obvious remedy is to improve the parallelism.

Mechanical tilt fluctuations:

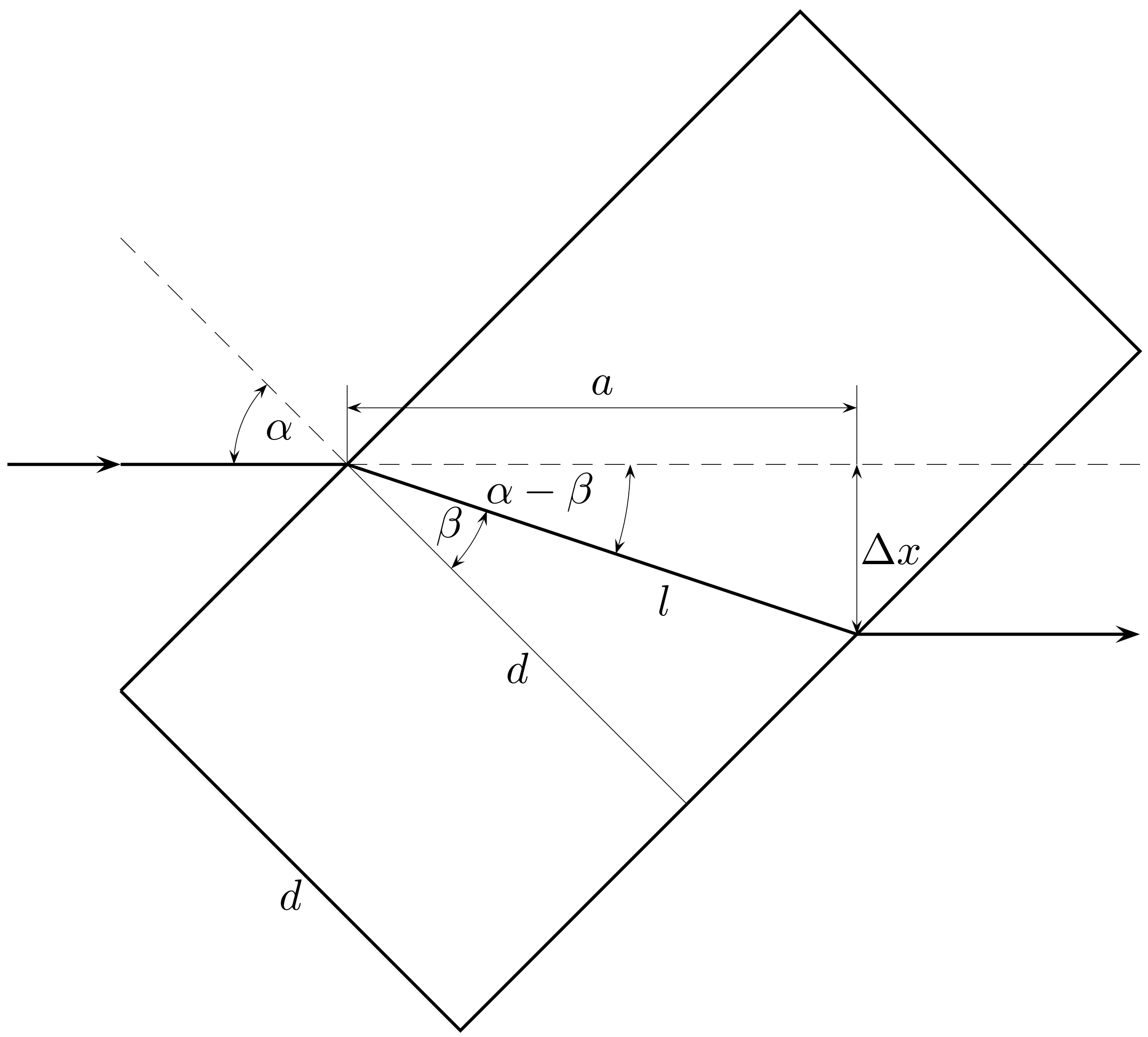

$$l = \frac{d}{\cos\beta}\,,$$

$$a = l\cos(\alpha-\beta),$$

$$\frac{\sin\alpha}{\sin\beta} = n\,,$$

$$\Delta s = nl - a$$

$$\Delta s = d\left(\sqrt{\frac{\cos 2\alpha + 2n^2 - 1}{2}} - \cos\alpha\right)$$

With $\alpha = 2.5^\circ$, $d = 6\,\text{mm}$, $n = 1.6$:

$$\frac{d(\Delta s)}{d\alpha} = 0.98\cdot 10^{-4} \approx 10^{-4}\text{m/rad}$$

For a pathlength error of $0.16\,\text{pm}/\sqrt{\text{Hz}}$ ($0.33\,\text{pm}/2$ because of double-pass) one gets

$$\widetilde{\delta\alpha} < 1.6\,\text{nrad}/\sqrt{\text{Hz}}.$$

If too difficult, α might be reduced at the expense of stray light problems.

Functional, environmental and performance tests

The EM was tested during March and April, 2004 at TNO/TPD, Delft. The tests included:

- Functional tests before and after each other test,
- Thermal vacuum test:
  several cycles 0...40 °C,
- Vibrational test (with dummy masses):
  8 g_{rms} sine and random,
  25 g at the struts.
- Performance tests:
  - Full stroke test: each mirror moved by $\pm 100\,\mu$m,
  - Noise test: mirrors not actuated
  - Tilt test: each mirror tilted by $\pm 1000\,\mu$rad,

All tests were successful!

EM Test results: high velocity full stroke test (2.9 samples/cycle)

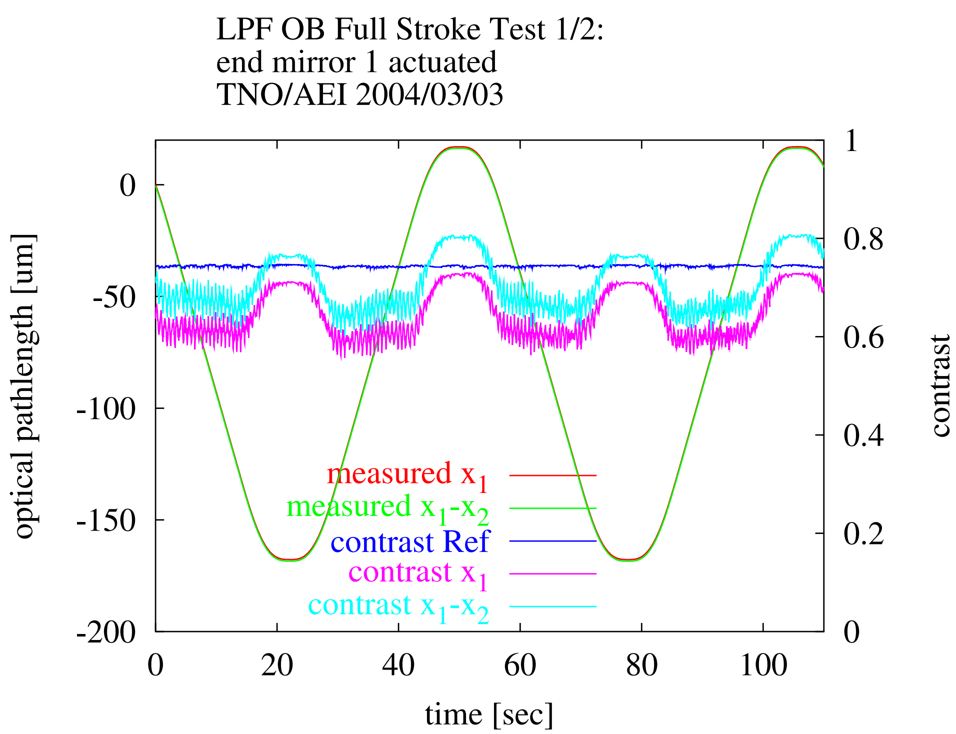

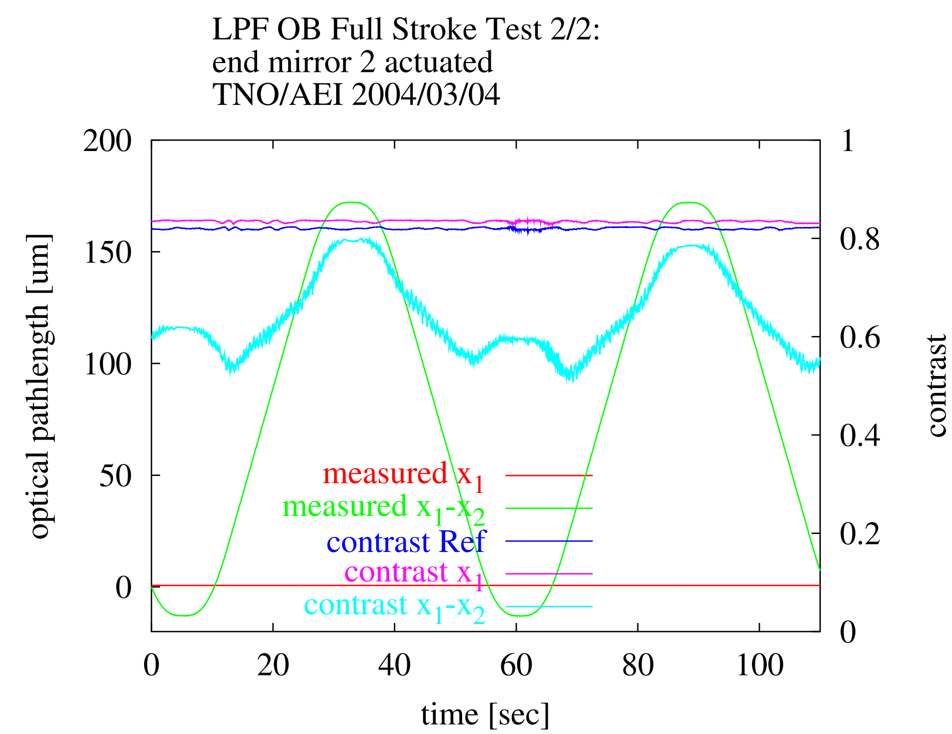

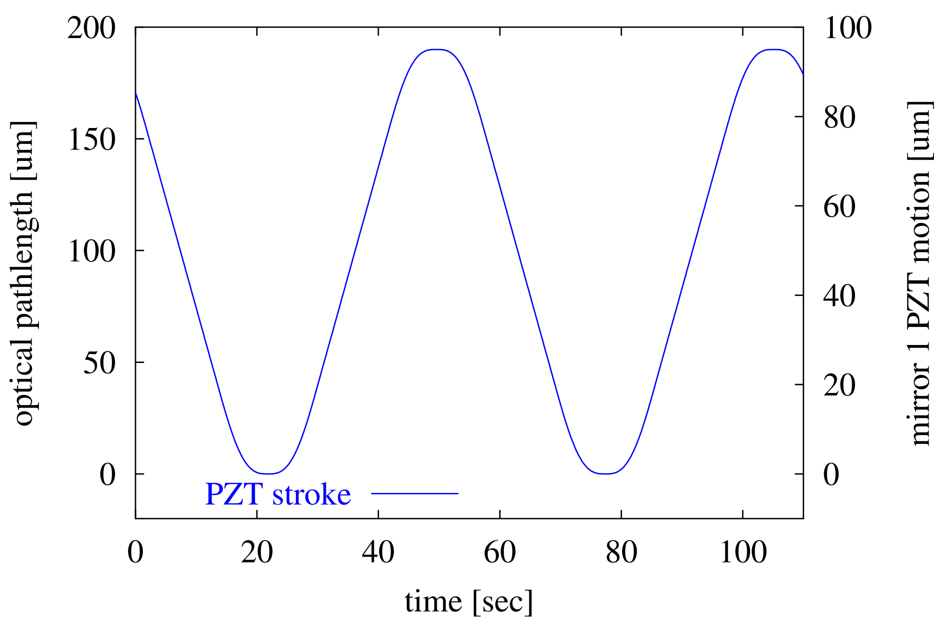

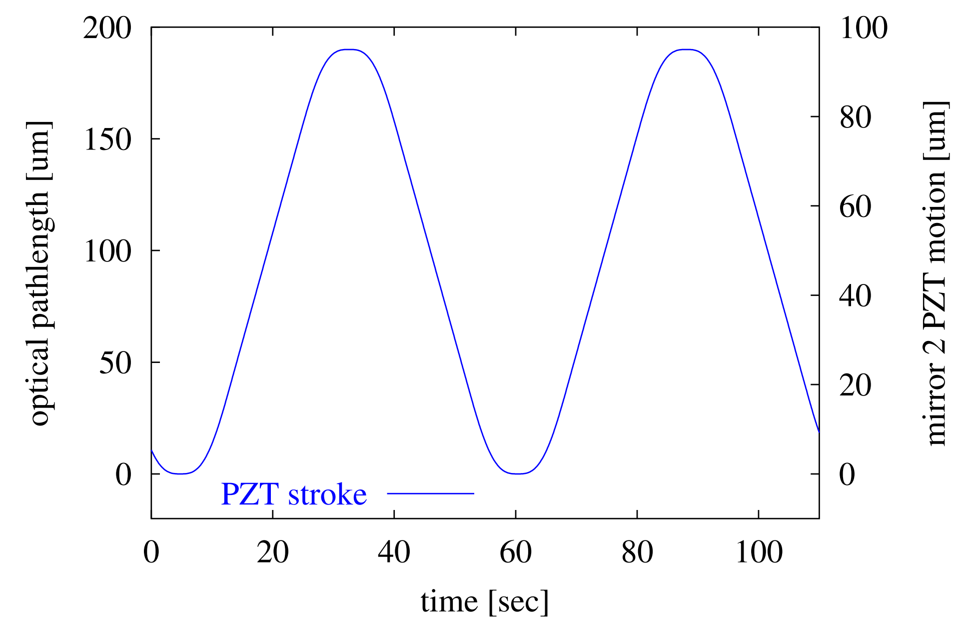

EM Test results: Noise

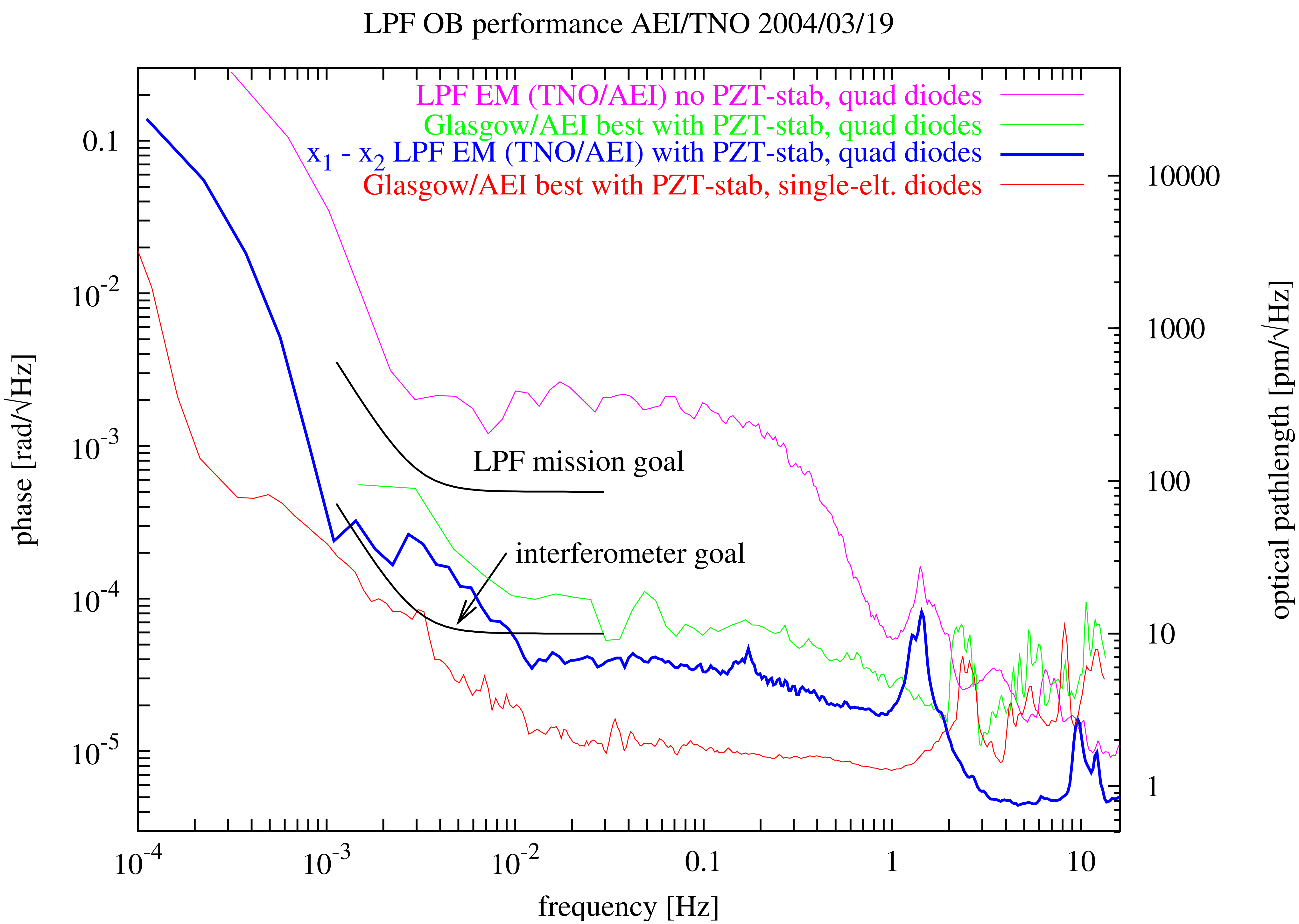

EM Test results: Contrast

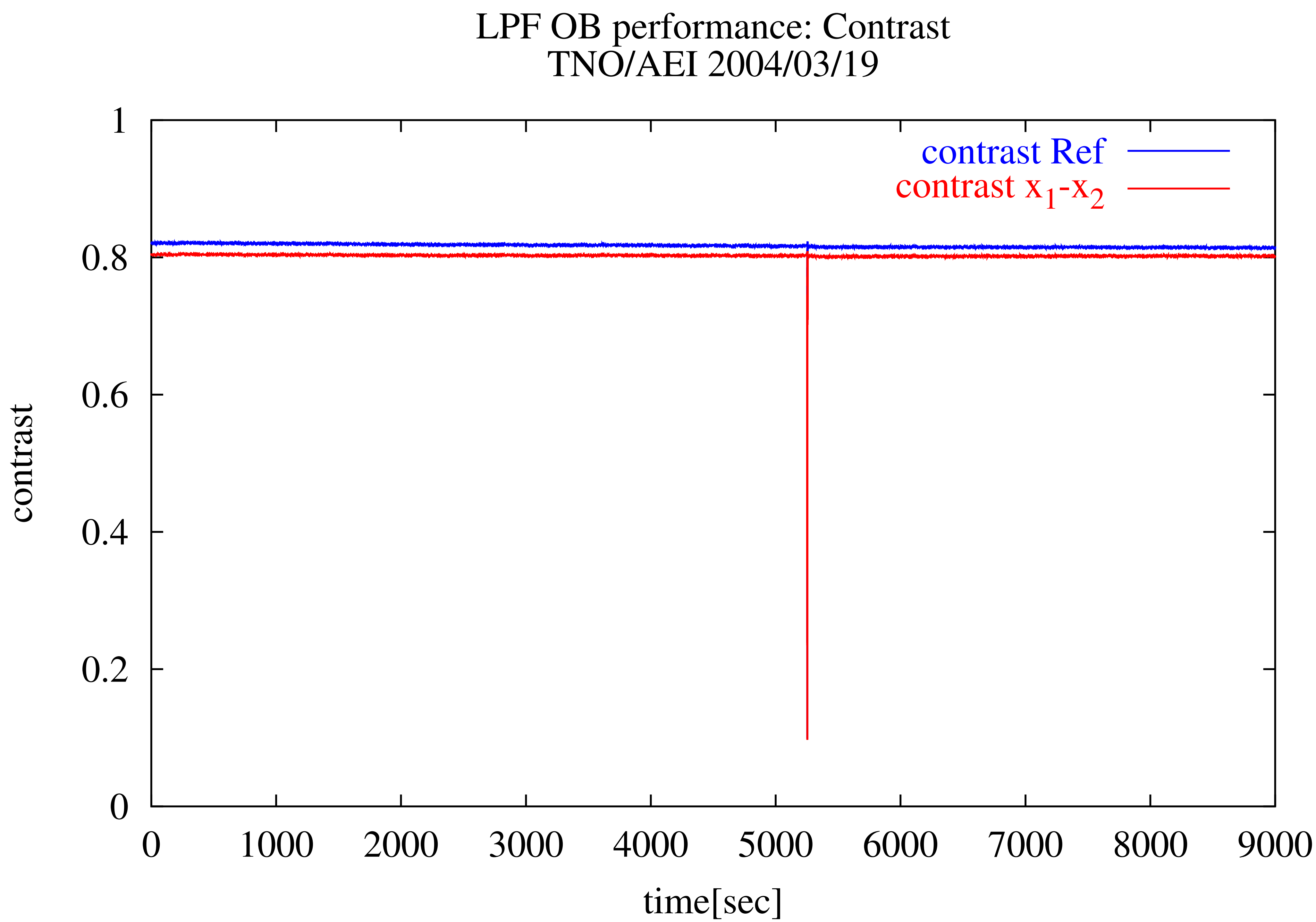

EM Test results: Noise sources 1

At frequencies $< 3\,\text{mHz}$, real motion of the test mirrors is dominant:

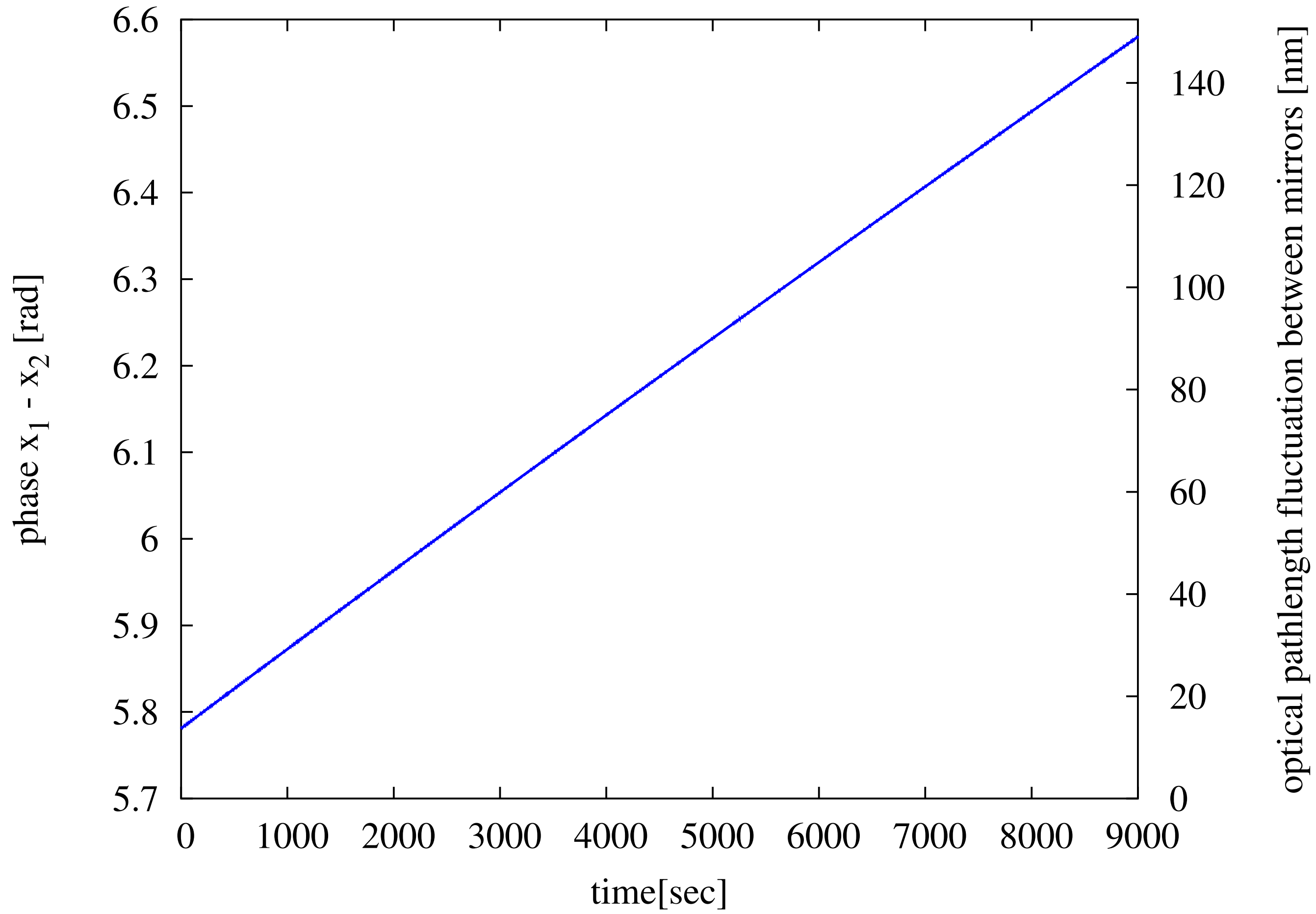

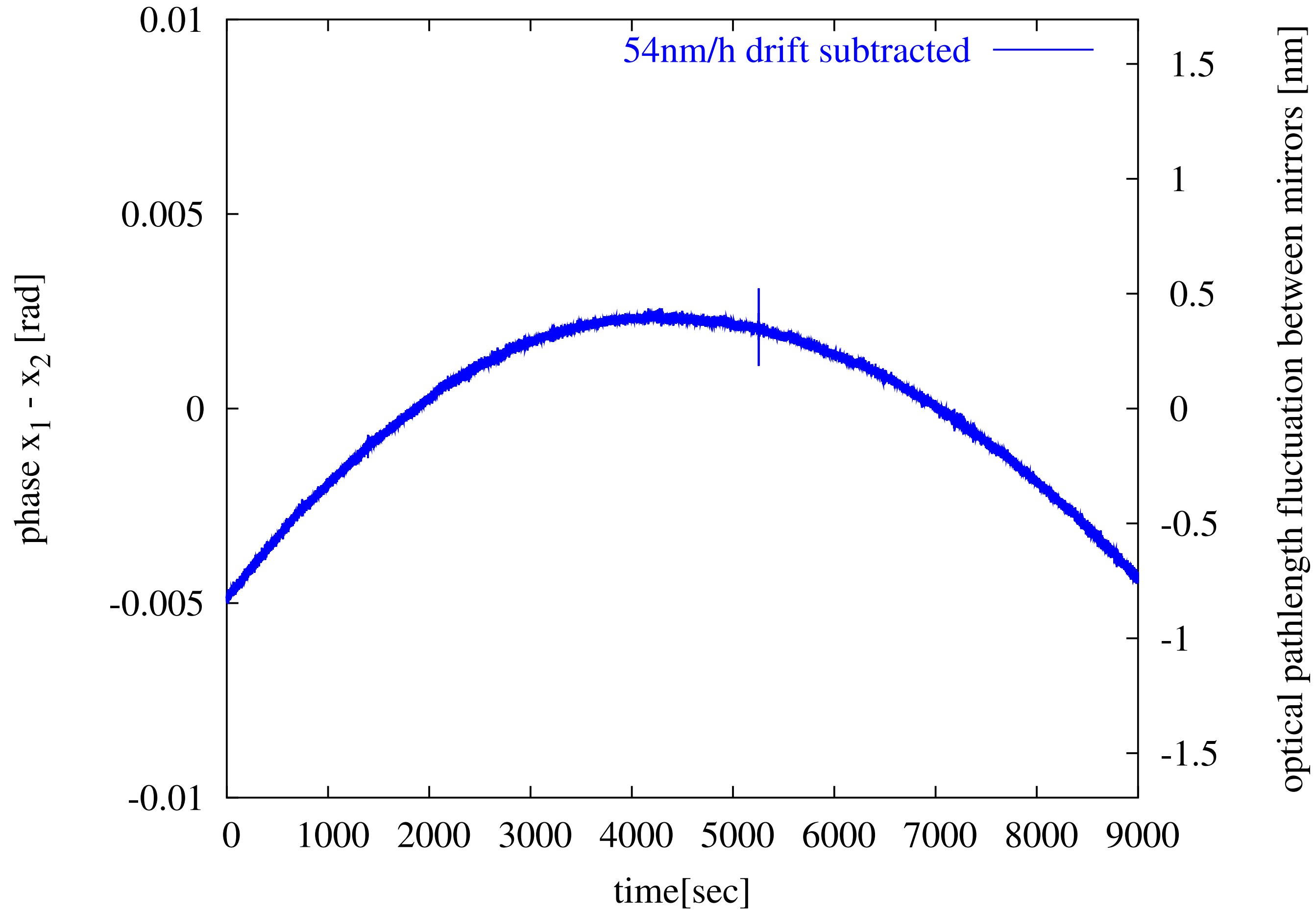

EM Test results: Noise sources 2

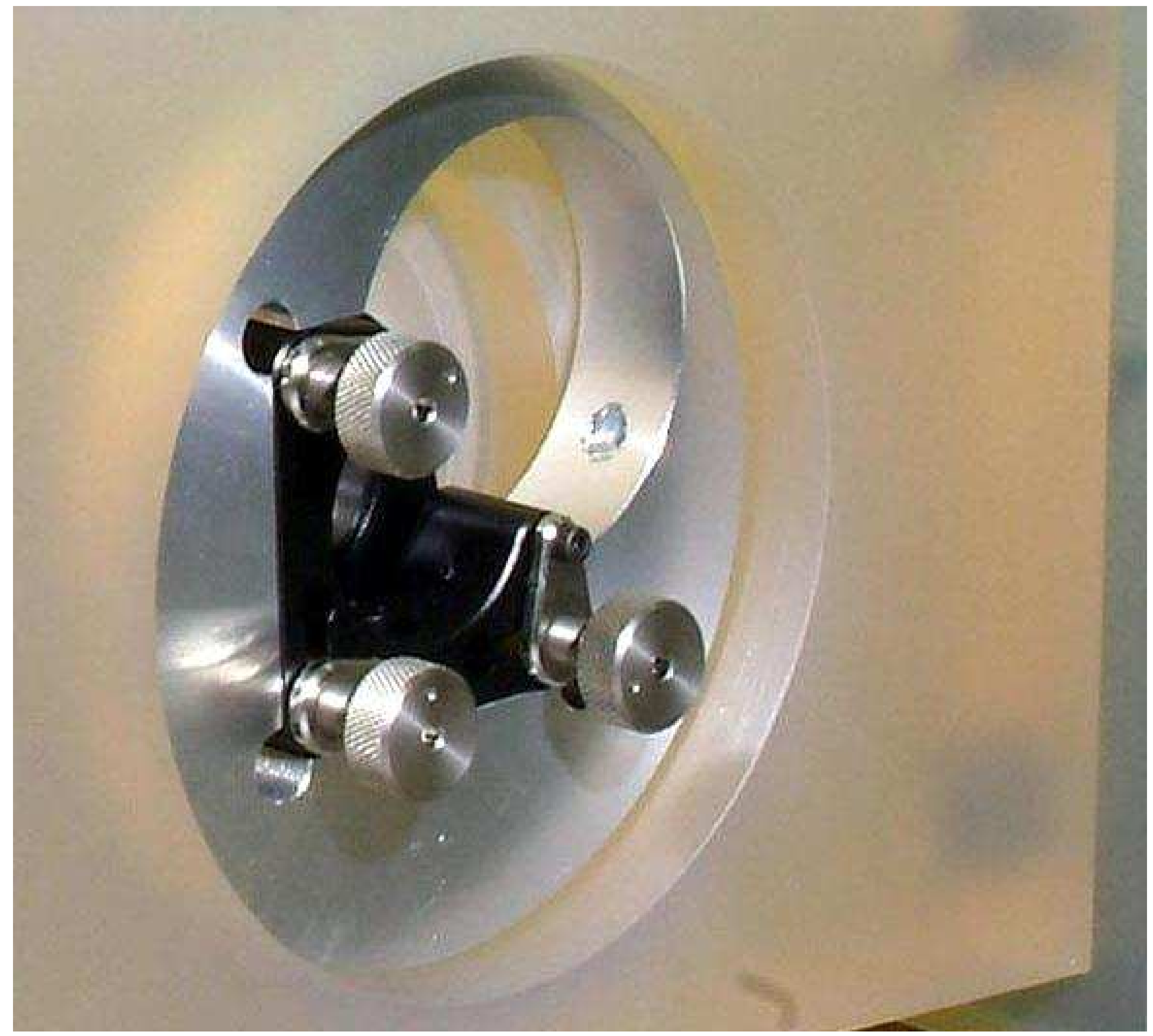

An attempt to glue the Zerodur mirrors to the Zerodur baseplate failed: Curing of the glue caused $\approx 200\,\mu$rad misalignment and a contrast drop to < 0.5. This is mainly a testing problem.

EM Test results: Noise sources 3

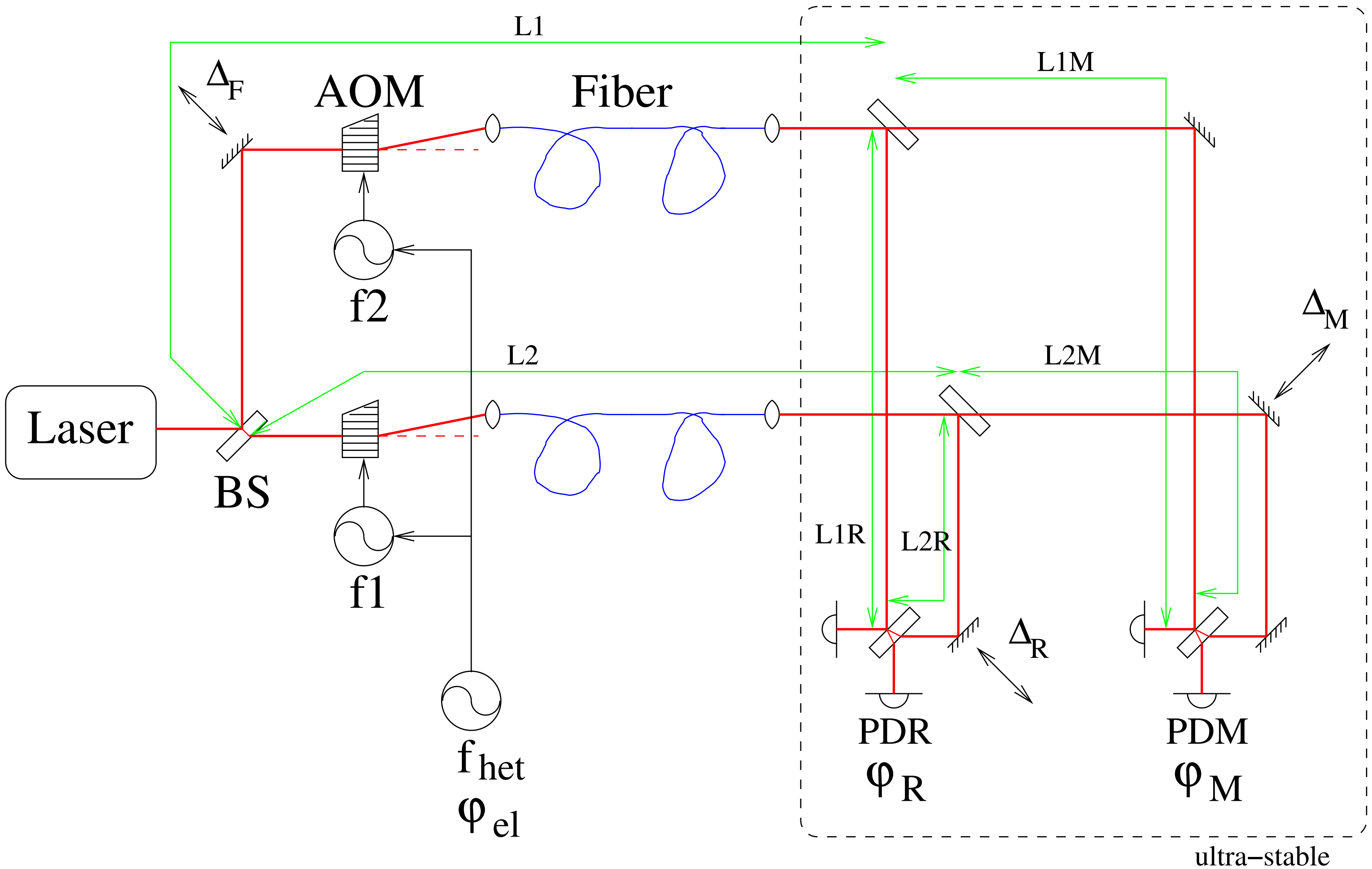

Fluctuations of the fibers' Optical Pathlength Difference (OPD, Δ_F) should ideally completely cancel, but in reality some error remains.

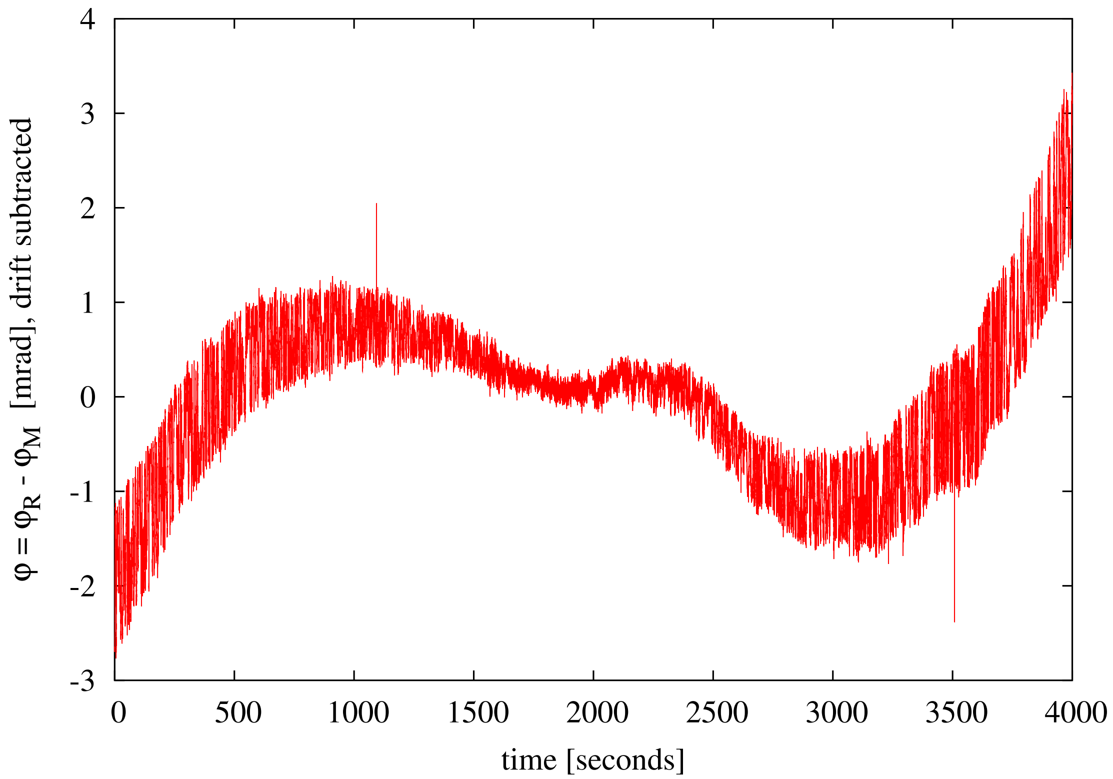

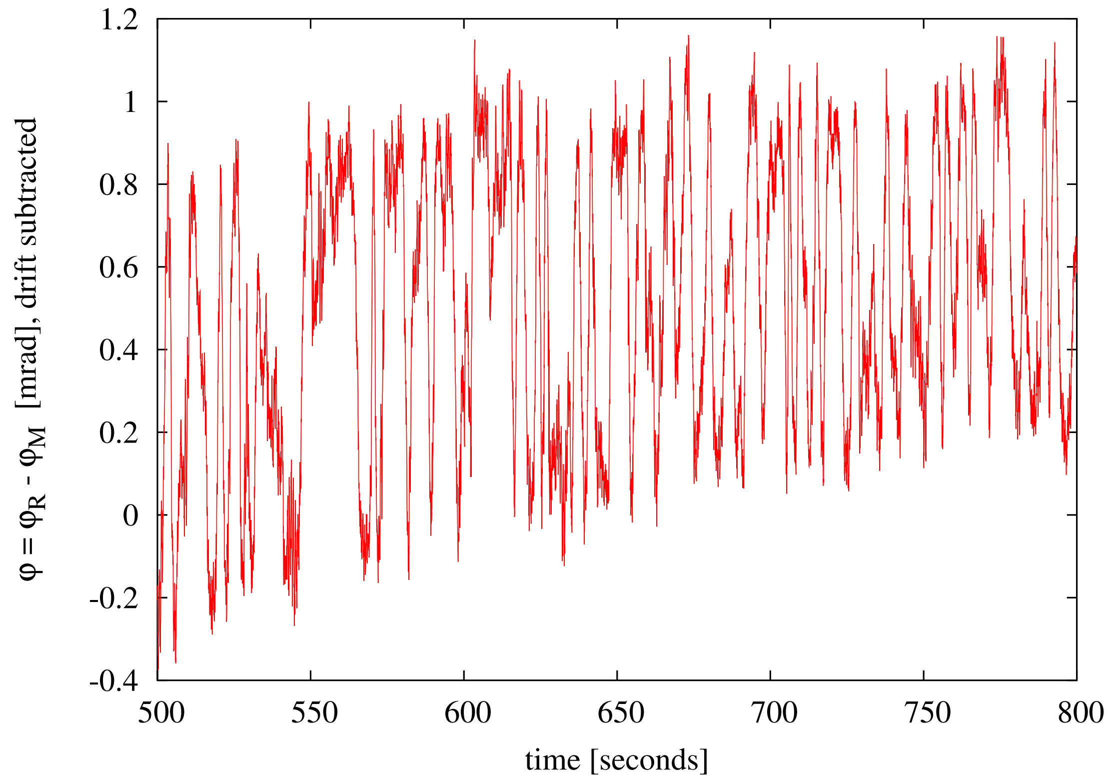

The measured pathlength $x_1 - x_2$ signal has an erroneous component of $\approx$ mrad magnitude which is quasi-periodic with Δ_F.

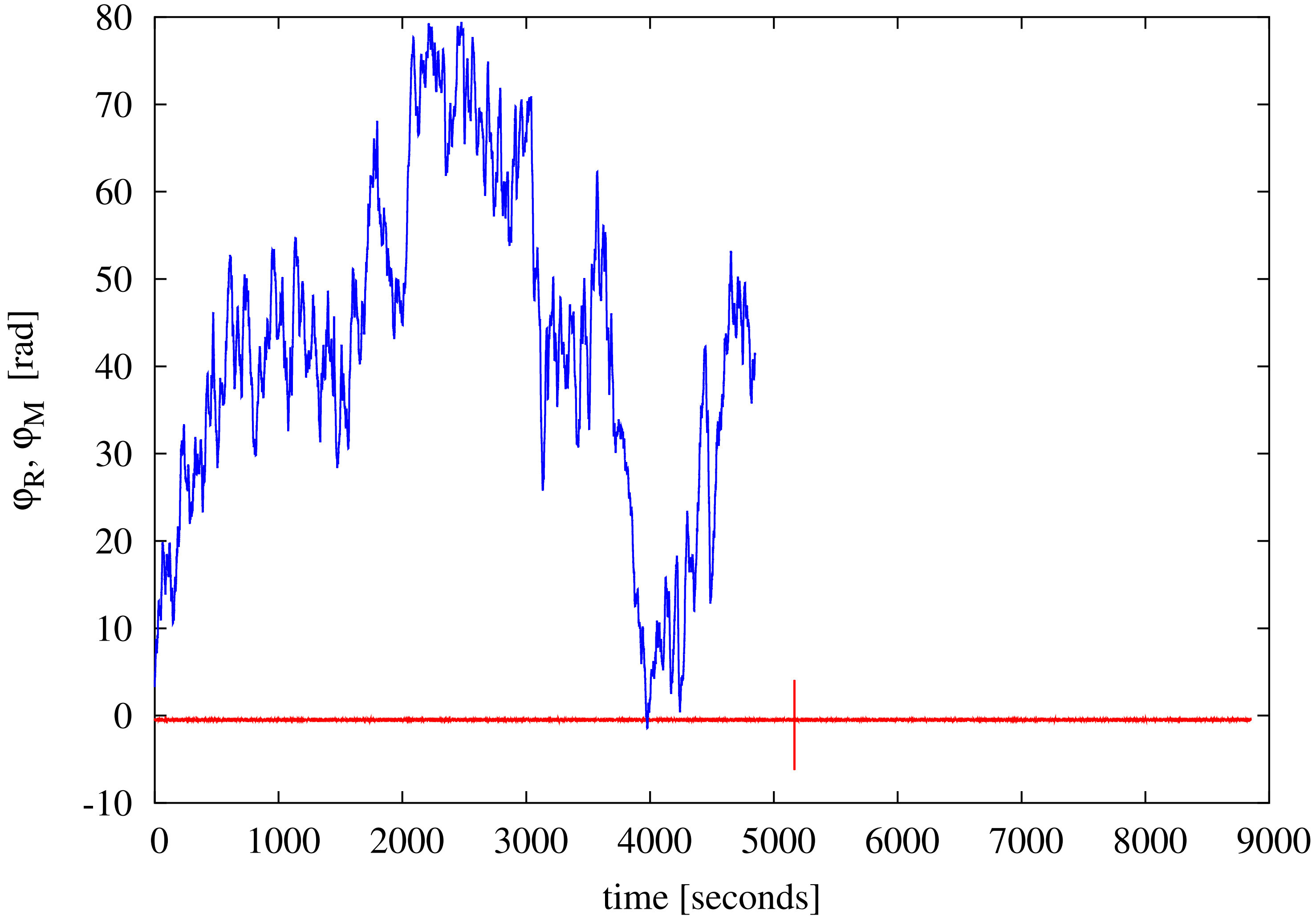

Unless the origin of the noise will be understood, a remedy is to actively stabilize Δ_F. This was done using an analog phasemeter, analog servo and long-range PZT at TNO.
Further investigations are under way in Hannover and Glasgow.

Alignment measurement with quadrant photodiodes

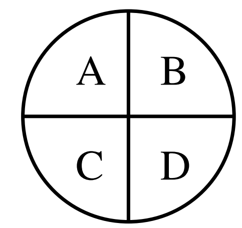

3 ways to use a quadrant diode:

- $\Sigma = A + B + C + D$ is used as before for the longitudinal readout.
- The DC signals $\Delta y = A + B - C - D$ and $\Delta x = A + C - B - D$ measure the **average lateral displacement** of both beams.
- Differential wavefront sensing measures the **angle between interfering wavefronts:**

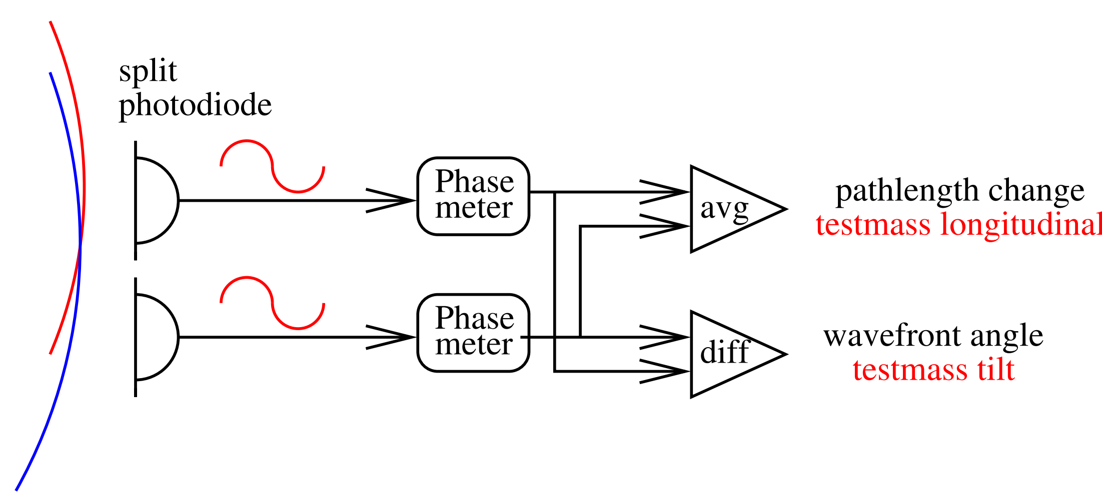

tilt test: mirror 1 x (horizontal)

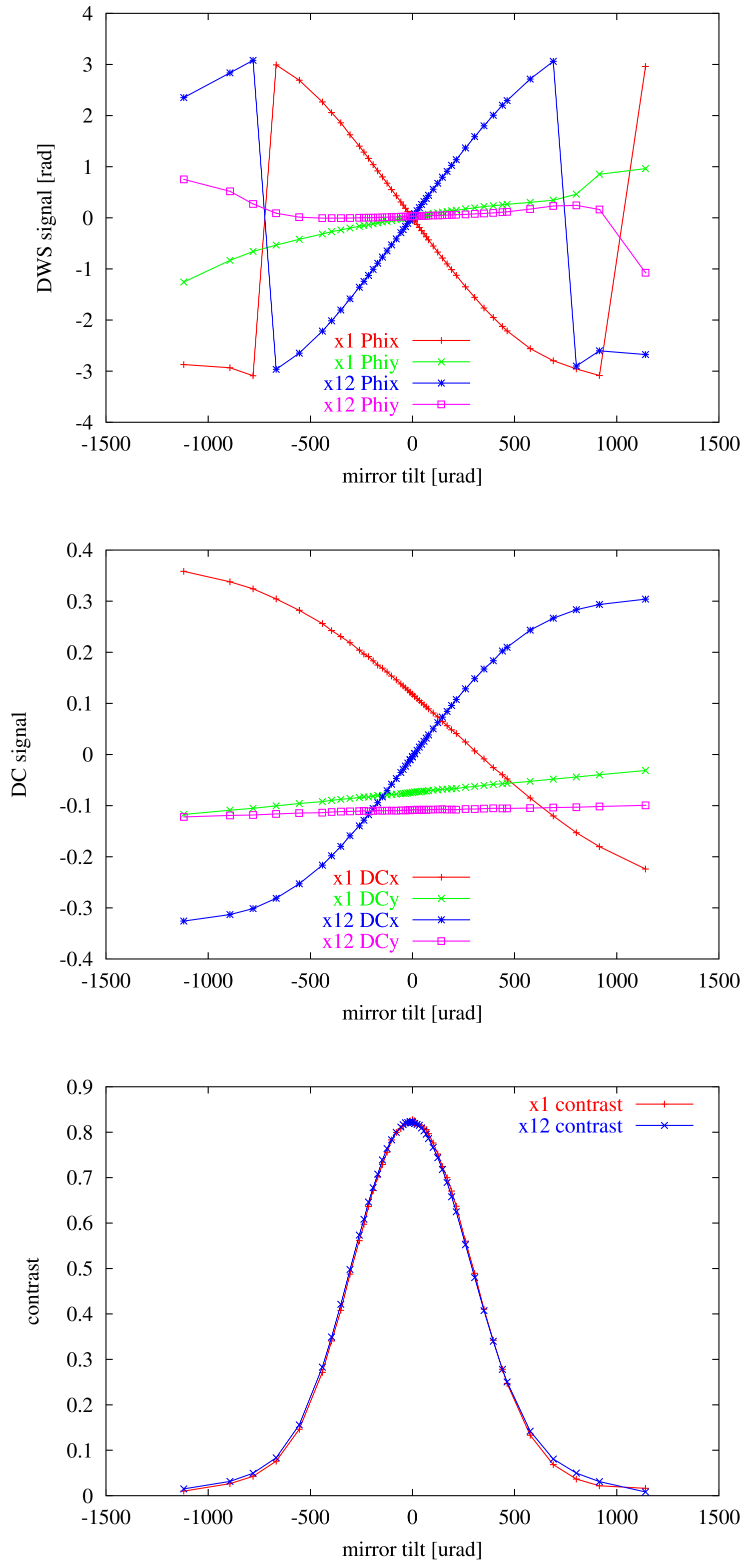

tilt test: mirror 2 x (horizontal)

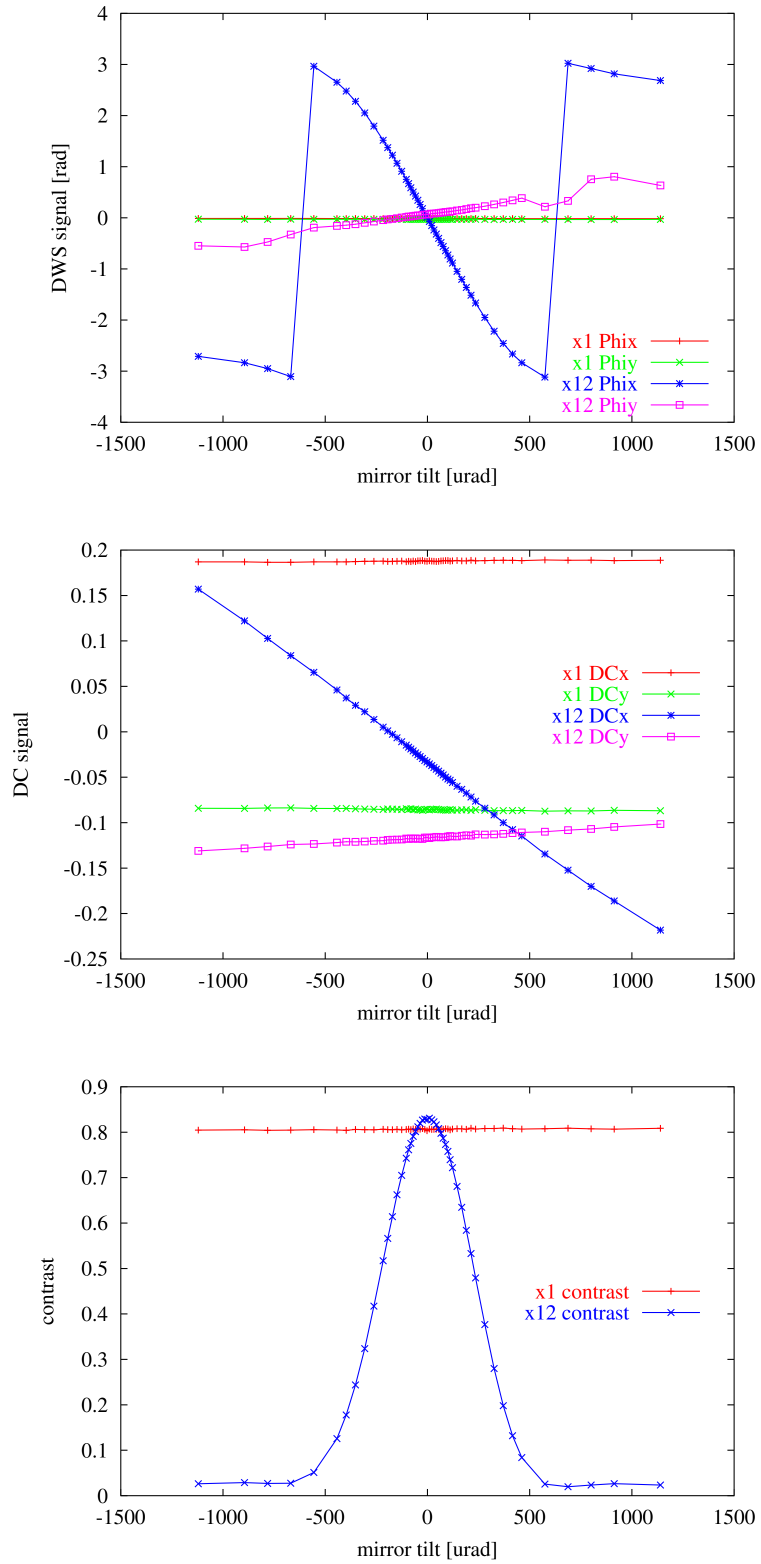

EM Test results: DC alignment signals

The calibration factor from test mass tilt angle α to Δx is (with several idealizations) given by $d(\Delta x)/d\alpha = 2\sqrt{2/\pi}\, L/w$, where $L \approx 25\ldots50\,\text{cm}$ is the lever arm from test mass to photodiode, and $w \approx 0.5\ldots1\,\text{mm}$ the beam radius at the photodiode.

	Rot. TM1	Rot. TM2	units
x_1 ifo predicted (numerical)	759	0	1/rad
x_1 ifo measured (x)	357	0	1/rad
x_1 ifo measured (y)	310	0	1/rad
$x_1 - x_2$ ifo predicted (numerical)	1147	304	1/rad
$x_1 - x_2$ ifo measured (x)	537	180	1/rad
$x_1 - x_2$ ifo measured (y)	468	184	1/rad

- conversion factor depends on beam parameters and beam power ratio (unbalanced during this measurement).

- DC alignment signals have higher noise than DWS signals.

- DC alignment signals are used for rough alignment of test mass when DWS contrast is insufficient.

EM Test results: DC alignment signals

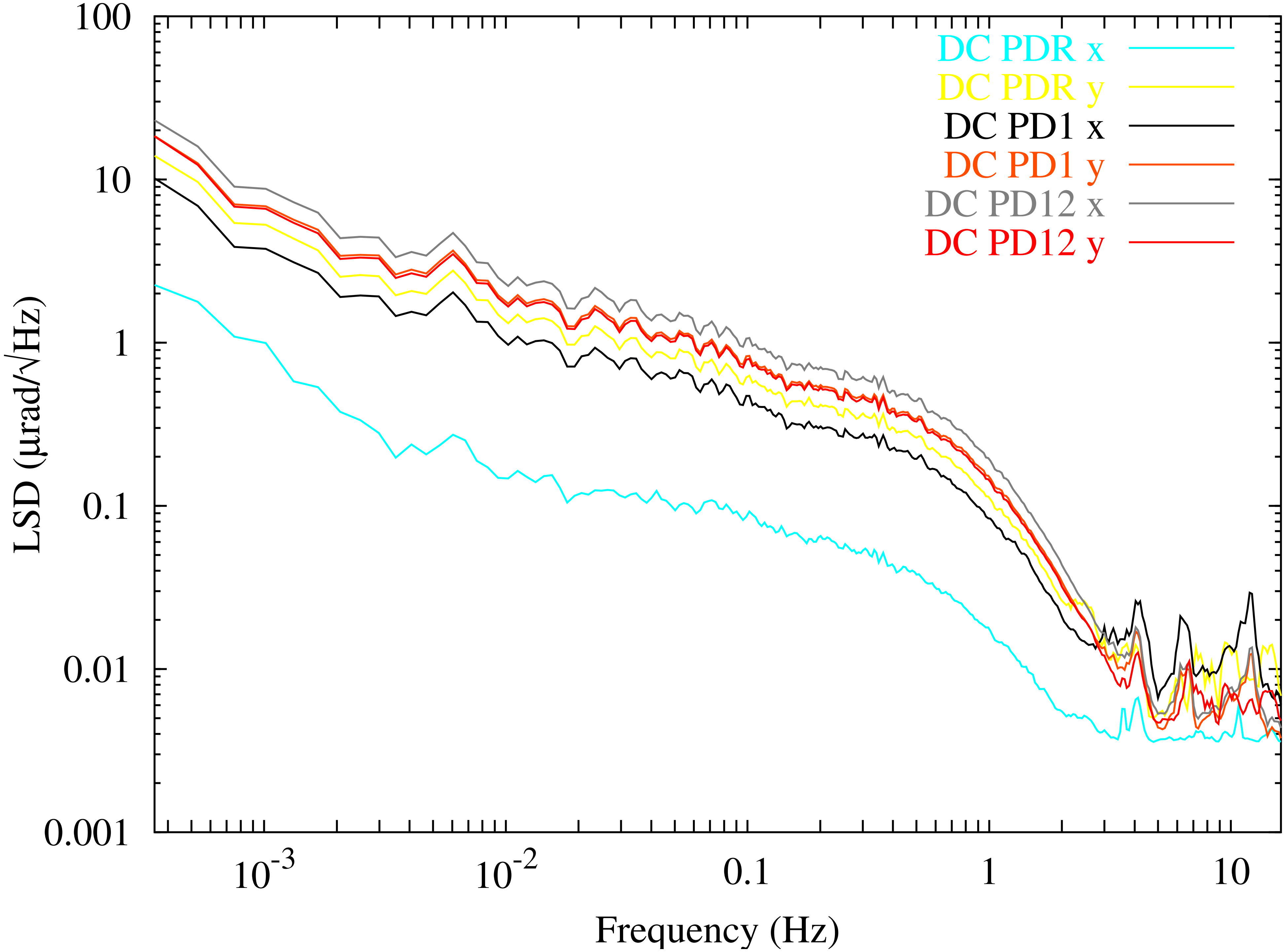

EM Test results: Differential wavefront sensing (DWS)

The conversion factor of test-mass angle α to (differential) phase readout φ is analytically:

$$\varphi/\alpha = 2\sqrt{2\pi}w(z)/\lambda \approx 5000\,\text{rad/rad}.$$

	Rot. TM1	Rot. TM2	units
x_1 ifo predicted (numerical)	5337	0	rad/rad
x_1 ifo measured (x)	5441	0	rad/rad
x_1 ifo measured (y)	5167	0	rad/rad
$x_1 - x_2$ ifo predicted (numerical)	4963	5994	rad/rad
$x_1 - x_2$ ifo measured (x)	5365	7263	rad/rad
$x_1 - x_2$ ifo measured (y)	5072	6940	rad/rad

- conversion factor depends on beam parameters; calibration is necessary.
- Better than the angular readout capability of the capacitive sensors; will be used to stabilize the alignment of the test masses.
- DWS works only when there are fringes (test mass absolute alignment better than 300 μrad). Otherwise, DC alignment signals are used for rough alignment of test mass.

EM Test results: Differential wavefront sensing (DWS)

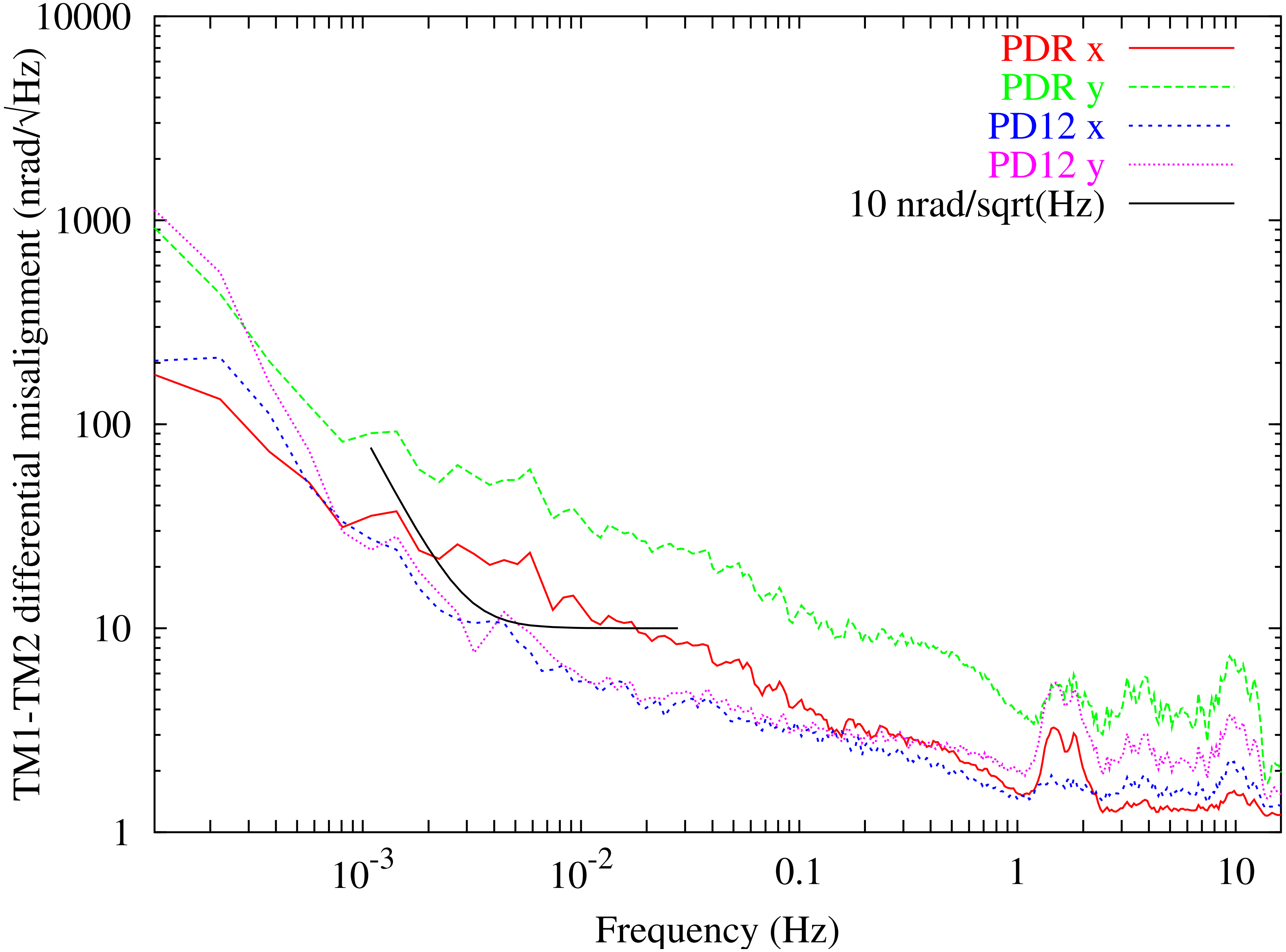

Summary

- interferometry and phase measurement for LTP work as predicted.
- some minor refinements are needed in the construction procedure.
- environmental and performance testing was successful.
- further investigations will concentrate on the ‘small vector’ noise.